Epibenthic megafauna associated with sponge grounds formed by the unique glass sponge *Vazella pourtalesii* in Emerald Basin, Nova Scotia, Canada

Nickolas J. Hawkes

Thesis submitted in fulfilment for the degree of Master of Science

Department of Biology

University of Bergen

July 2017

Table of Contents

Acknowledgements

I would like to thank my amazing supervisors Hans Tore Rapp, Ellen Kenchington and Joana Xavier. I am a person who leaves things to the last minute in an almost pathological fashion, yet you all offered help and support throughout the entire span of the master project. I am deeply grateful that I was fortunate enough to have all of you as my supervisors. Thank you to the extremely welcoming Marine Biodiversity Group!

The scientific cruise onboard the CCGS Hudson was an extremely giving experience. Although Lindsay Beazley was technically not my supervisor you were probably the person I asked the most when I needed help and your responses were always prompt, despite the time differences between Canada and Norway.

A big thank you to Michelle Korabik. You are one of the most friendly people I have ever met and guided me through your own project step by step with tremendous patience. The impetus for this master project would have never been there in the first place without your hard work, so I am in your debt. I also now seem to find Unidentified 33s wherever I go, which could be associated with the hair loss that came as a result of this master project (I'm only joking).

Thank you to all of the wonderful people at the DFO: Robert Benjamin, Igor Yashayaev, Emily Baker, Javier Murillo, Sarah, Cam and Barry.

For all your knowledge on statistics and the importance of asking the right questions, thank you Knut Helge Jensen.

My final thanks goes to my friends, sponge family and family. Your support helped carry me through the entire master project.

Abstract

Large, dense aggregations of sponges or “sponge grounds” have seen a surge of scientific interest in recent years. The pivotal ecological functions of sponges may warrant conservation measures that have been neglected in the past. The slow growth and low recovery potential of some deep-sea sponges, combined with their fragile morphologies, contributes to vulnerability to mobile fishing gear, particularly bottom trawling. The largest monospecific aggregation of *Vazella pourtalesii*, the Russian hat, was recently described off the Scotian Shelf between 75-275 m depth, extending over 8,500 km^2. Here I describe and compare the epibenthic megafauna inside and outside sponge grounds, and, if the condition (live, dead and damaged) of *Vazella pourtalesii* has an effect on the local biota and its composition. Building on previous work, I also account for the effect of substrate to see if *Vazella pourtalesii* enhances local biota, as previous work has shown. The results suggested that *Vazella pourtalesii* had a positive influence on local epibenthic megafauna, as well as the community compositions; however, more data is needed to provide a complete answer. This research will aid managers in the future, by helping to untangle the intricacies of this interesting habitat so as to avoid further significant adverse impacts.

Introduction

Sponges are common but often underappreciated (Bell, 2008), members of both freshwater (Manconi & Pronzanto, 2008) and marine benthic communities (Maldonado *et al*., 2016). Monospecific (e.g. Fuller, 2011) and multispecific (e.g. Klitgaard & Tendal, 2004; Murillo *et al.*, 2012) sponge aggregations (commonly referred to as sponge grounds) are found at virtually all depths and encompass a wide range of habitats from the intertidal (Lysek *et al*., 2003); to abyssal depths of the deep-sea, where in some instances sponges account for roughly 90 % of the sessile biomass (Maldonado *et al.*, 2016). Sponges also have an extensive geographic distribution, from the highly diverse coral reef sponges in the tropics (e.g. Diaz & Rützler, 2001), to the sponge grounds at higher latitudes: astrophorid demosponges of the North-Atlantic (Klitgaard & Tendal, 2004; Murillo *et al*., 2012); and, the extensive sponge grounds of the Antarctic continental shelf (Kersken, Feldmeyer & Janussen, 2016). Sponges also display a wide range of modes to obtain energy: (i) the more common heterotrophic species that are benthic suspension feeders; (ii) "autotrophic" sponges that can obtain at least part of their energy from sunlight due to photosynthetic endosymbionts, for example, dinoflagellates of the genus *Symbiodinium* (Fang *et al*., 2017); and finally, (iii) sponges of the Family *Cladorhizidae* that have partly or completely reduced their aquiferous systems, and instead derive energy from captured epibenthic organisms (Hestetun *et al.*, 2016; Goodwin *et al*., 2017). Although fields such as sponge taxonomy and systematics are constantly evolving (Wörheide *et al.*, 2012; Cárdenas, Pérez & Boury-Esnault, 2012), much remains unresolved, such as the on-going research in the skeletal evolution of glass sponges (Dohrmann *et al.*, 2017). A comparative trend is also reflected in the ecological research on sponges (Bell, 2008; Maldonado *et al.*, 2016).

Sponges are emerging as crucial components of marine systems (Maldonado *et al.*, 2016), with properties that emphasise them as ecosystem engineers (Jones, Lawton & Shachak, 1994), i.e., organisms that cause changes in the physical state of biotic and abiotic materials available to other species. Bell (2008) summarises three key ecological roles sponges play: (i) substrate modification and the hydrodynamics of the boundary layer, such as bioerosion and the stabilisation of sediment; (ii) a pivotal role in linking benthic and pelagic ecosystems, a phenomenon known as bentho-pelagic coupling, such as the biogeochemical cycling of silicon which traditionally only included diatoms and not siliceous sponges (López-Acosta, Leynaert & Maldonado, 2016); and, (iii) the ecological interactions and associations between sponges and other organisms (Wulff, 2006), such as the provision of micro- (e.g. Costa, Mansur & Leite, 2015) and macro-habitats (e.g. Korabik, 2016). The latter ecological function (iii) also emphasises sponges as an important source of shelter and refuge for marine organisms (Wulff, 2006), for example fish of the genus *Sebastes* (Freese & Wing, 2003;

Fuller, 2011). Considering the important ecological functions sponges can have, it is only natural to ask the question: Would one therefore expect higher relative biodiversity in areas with sponges? This is clearly evident in the ecological literature (Hogg *et al.*, 2010; Maldonado *et al.*, 2016), as sponges, particularly in dense aggregations commonly referred to as sponge grounds, locally enhance biodiversity. Biodiversity can be linked to several components of a sponge such as volumetric (e.g. Padua, Lanna & Klautau, 2013; Erdman & Blake, 1987; Duarte & Nalesso, 1996), morphological (e.g. Klitgaard, 1995; Beazley *et al.*, 2013) and chemical (e.g. Huang *et al.*, 2008), complexity. It is also important to stress the two main dimensions of biodiversity relating to sponges: the complex and highly diverse, microbiota within the sponge itself (Thomas *et al*., 2016), and, the observable megafauna associated with sponges (e.g. Beazley *et al*., 2013; Beazley *et al.*, 2015).

Whilst the individual characteristics of sponges can enhance local biodiversity, beneficial effects can be even greater in sponge grounds (Hogg *et al.*, 2010; Bo *et al.*, 2012). Sponge grounds not only enhance biodiversity due to the higher biomass or density of sponges, but with successive generations over time, spicules can accumulate to create dense "spicule mats" with profound beneficial effects on the local biodiversity, distribution of species and compositions of resident communities (Bett & Rice, 1992; Barrio Froján *et al.*, 2012; Gutt, Böhmer & Dimmler, 2013). The factors that drive the high density of sponges found in sponge grounds are not well known (but see Knudby, Kenchington & Murillo, 2013; Beazley *et al*., 2015); however, currents that bring food and nutrients down to these environments, and the transportation by the benthic boundary layer (i.e. the water and sediment immediately adjacent to the seafloor) are pivotal facilitators (Buhl-Mortensen *et al*., 2010). As the general trend is that habitat complexity and food supply decline with increasing depth (Buhl-Mortensen *et al.*, 2010), sponge grounds represent locally enhanced areas of biodiversity (Maldonado *et al*., 2016). The associations with commercial fish species (e.g. Fuller, 2011; Freese & Wing, 2003; Cook, Conway & Burd, 2008), pharmaceutical potential (e.g. Lind *et al.*, 2013; Manconi & Pronzanto, 2008) ecological functions (Bell, 2008) and the combined vulnerability and slow recovery of sponge grounds from damage caused by fishing gear (Freese *et al*., 1999; Freese, 2001; Cook, Conway & Burd, 2008), warrant powerful impetuses for the conservation of sponge grounds.

The unique *Vazella pourtalesii* sponge grounds in the Emerald Basin (extending over 8,513 km^2) which are the focus of this thesis, were first scientifically described by Fuller *et al.* (2008) and more extensively by Fuller in 2011; however, Fuller noted that fishermen were aware of it at a far earlier date, as it "filled the nets" (Fuller, 2011) when targeting redfish (*Sebastes spp.*) and pollock

(*Pollachius virens*). *Vazella pourtalesii* (Schmidt, 1870), commonly known as the "Russian hat", is a glass sponge of the Class Hexactinellida, with typical six-rayed, or "hexactine" silica spicules. It is a member of the Family *Rosselidae* (Reiswig, 2006) and may be closely related to *Symplectella rowi,* although this is not significantly supported (Dohrmann *et al.*, 2017). It was previously only known in small aggregations and comparatively smaller specimens in the Azores and Gulf of Mexico, with the latter location also being the location of the type specimen (Fuller, 2011). Growth rates are unknown and only inferred from related species, and may be on the order of centimetres per year; however, it was found to range from 2 to 110 cm in height and 2 to 75 cm in width from video analyses (Fuller, 2011). *Vazella pourtalesii* is a large, vase-shaped sponge, with a single large osculum and body cavity. Large spicules extend out of the exterior of sponge, which often accumulate flocculent material in clumps, as noted by Fuller (2011) and Korabik (2016). The *V. pourtalesii* sponge grounds were declared a vulnerable marine ecosystem (VME) by the Northwest Atlantic Fisheries Organization (NAFO, 2009) and later a Sensitive Benthic Area (DFO, 2014). The research conducted on the *Vazella pourtalesii* sponge grounds (Fuller *et al*., 2008; Fuller, 2011; Kenchington *et al.*, 2010) as well as Fisheries and Oceans Canada (DFO) research trawls, resulted in protective action being taken. Two areas with restrictions to bottom trawling were established in the Emerald Basin (197 km^2) and Sambro Bank (62 km^2) in 2013 (DFO, 2014), under the DFO 2009 Policy for Managing the Impacts of Fishing on Sensitive Benthic Areas.

Although previous work has described and given an insight into the distribution (Fuller, 2011) and vulnerability (Fuller *et al.,* 2008) of the *Vazella pourtalesii* sponge grounds, only Korabik's image analysis (2016) has specifically looked at small scale associations between *Vazella pourtalesii* and epibenthic megafaunal composition and biodiversity. Areas with *V. pourtalesii* present had higher biodiversity and abundance, as well as different community compositions of epibenthic megafauna than areas without *V. pourtalesii* (Korabik, 2016). The condition of *V. pourtalesii* also showed (ANOVA) differences in the biodiversity and abundance of epibenthic megafaunal communities, with the highest biodiversity found in areas with mixed (i.e. combinations of either live, dead or damaged individuals) assemblages of *V. pourtalesii*. Statistically significant differences in the community compositions were found between the different assemblages; however, similar species existed in both assemblages and the average differences were of relatively low magnitude. Because of the interesting trends and research by Korabik (2016), I wish to examine the nature of these patterns in more detail: (i) examining if *V. pourtalesii* can predict differences in biodiversity, accounting for the likely non-normal distribution and potential heteroscedasticity of the data (see O'Hara & Kotze, 2010); (ii) including the effect of transects as random intercepts, i.e. a generalised linear mixed

model (GLMM) approach (Bolker *et al*., 2009); and, (iii) analysing the potential effect that substrate (measured as percentage coverage of hard substrate) may have on biodiversity (e.g. Lacharité & Metaxas, 2017). I hypothesise on similar grounds to Korabik (2016) that: (i) the biodiversity and abundance of epibenthic megafauna will be highest in areas with *V. pourtalesii* present; and, (ii) that biodiversity and abundance of epibenthic megafauna will be higher in areas with mixed or live assemblages of *V. pourtalesii* than areas with solely dead assemblages. Finally (iii), with the inclusion of substrate as a predictor of biodiversity and abundance, I hypothesise that increases in the percentage coverage of hard substrate will have a positive effect on biodiversity and abundance, as this also corresponds to higher habitat heterogeneity and complexity. Epibenthic megafauna were defined as organisms ≥ 1 cm, motile or sessile, living on or near the seafloor (*sensu* Korabik, 2016; Beazley *et al.*, 2013; 2015; Beazley & Kenchington, 2015).

Methods

Study area

The Scotian Shelf is a 700 km long section of the continental shelf off Nova Scotia, and is bounded by the Northeast Channel to the south-west and the Laurentian Channel to the north-east (Shaw *et al.*, 2006). The Emerald Basin is one of the largest of a series of irregular basins off the Scotian shelf, approximately 60 nautical miles south of Halifax, Nova Scotia (Fig. 1). The geological features and hydrographic properties of the area have been sampled and studied extensively previously (Keigwin, Sachs & Rosenthal, 2003). The Emerald Basin is characterised by thick post-glacial sediments (King & Fader, 1986).

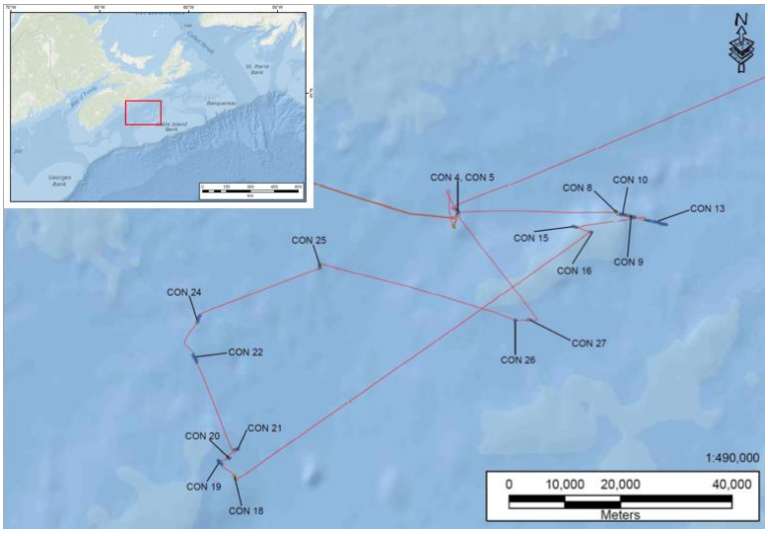

Fig. 1. Map of the 2011 CCGS *Hudson*'s cruise track to Emerald Basin off the Scotian Shelf. All 17 transects (Consecutive Operations Numbers, CON) are shown. The area of the main figure is shown in a wider extent in the figure in the top-left corner.

Acquisition of underwater imagery

17 benthic imagery transects were collected by Fisheries and Oceans Canada (DFO) in the Emerald Basin during a cruise made onboard the Canadian Coast Guard Ship *Hudson*, in June 2011 (Fig. 1); as part of a research inquiry from the North Atlantic Fisheries Organization (NAFO) to scientifically assess the impacts of bottom trawling on vulnerable marine ecosystems (see Kenchington *et al.*, 2011). Transects were approximately a kilometre in length, however, some variation occurred due to differences in the magnitude and direction of wind speed and water currents. Images were obtained using the Campod Camera System, a lightweight tripod system controlled by a winch on deck, with an operative depth of approximately 650 m. The Campod Camera System housed three cameras, two which took continuous colour video footage: (i) an obliquely mounted Sony SC-999 camera for a forward-facing view of the seafloor and (ii) a Sony DXC-950 camera, mounted on the bottom of the Campod Camera System for a downwards-view of the seabed; and, (iii) a Nikon D300 camera with two high-speed flashes that took high-resolution (12 MP) digital stills. A temperature and pressure recorder (SBE39) was also attached to the Campod Camera System, as well as two lasers calibrated 10 cm apart that were used as a size reference. Images were taken once every minute, with the photographic unit of the Campod Camera System approximately one metre above seafloor. The video footage was not used directly in this study, but was used to map the distribution of *Vazella pourtalesii* in the 17 transects (DFO, unpublished data), and aided in the selection of transects for Korabik's work (2016) and this study. Five transects were analysed in this study, as indicated by their Consecutive Operation Numbers (CON, Table 1). CON 18, 19, 20 and 21 were selected due to their geographical proximity and representation of live, dead and damaged *Vazella pourtalesii*. CON 5 was selected due to its high densities and representation of live and dead *Vazella pourtalesii*.

Table 1.
Summary of the five benthic imagery transects sampled using the CCS in the Emerald Basin.

Transect	Position (dec. degrees)		Depth			Transect length (m)	Number images analysed	Total area covered (m^2)
	Start (°N/°W)	End (°N/°W)	Min (m)	Max (m)	Mean ± SD (m)			
CON 18	43.8677/-63.0630	43.8676/-63.0629	203.2	211.2	208.7 ± 1.7	924	60	24.1
CON 19	43.8836/-62.0910	43.8897/-63.1012	148.6	168.1	156.5 ± 5.9	1528	156	62.6
CON 20	43.8938/-63.0742	43.8961/-63.0837	151.4	173.5	159.2 ± 5.7	926	121	48.6
CON 21	44.9108/-63.0570	43.9076/-63.0673	210.0	226.0	221.0 ± 4.6	1034	78	31.3
CON 5	44.3136/-62.6065	44.3117/-62.6040	180.5	190.9	185.6 ± 3.3	780	52	20.9
Summary			148.6	226.0		1038.4	467	187.5

Underwater imagery annotation

A grid of 4 x 3 cells (A-L) and, scale bars of 1 cm within each of the grid cells was placed over each image using batch processing in Adobe Photoshop CS2 (Fig. 2), to ensure consistency in both the

quantification and identification of epibenthic megafauna within and among images. Standardised scale bars and the average area of each image were set by sampling 50 random photos across all 17 transects and measuring the number of pixels between the two laser points (10 cm). The CCS proved to be relatively stable at different depths across the transects, evident by the average number of pixels between the two laser points (Mean ± SD: 554.319 ± 33.367 pixels per cm), which translated into a relatively consistent area (Mean ± SD: 0.401 ± 0.0432 m^2). Photos that were too close or too far from the seafloor were excluded if the discrepancy between the scale bars and actual distance measured by the lasers was greater than 10%, as the area of these photos was significantly far off the average area used in the standardisation process in the analyses. A depth protocol was created to account for size estimation errors relating to the Campod Camera System transitioning from hard to soft substrate, as this would occasionally result in the legs of the device digging into the substrate (L. Beazley, personal communication, email, 29 November 2016). It was a simple measure that compared the discrepancy between the calibrated lasers and the pixels. Photos that were: too close together (i.e. sharing a common area and megafauna); blurry, with sediment clouds that significantly impeded the identification of megafauna (excluded if the total area equivalent to three grid cells or more was impeded), or too dark (i.e. sum of dark areas spanning more than three grid cells), were also excluded.

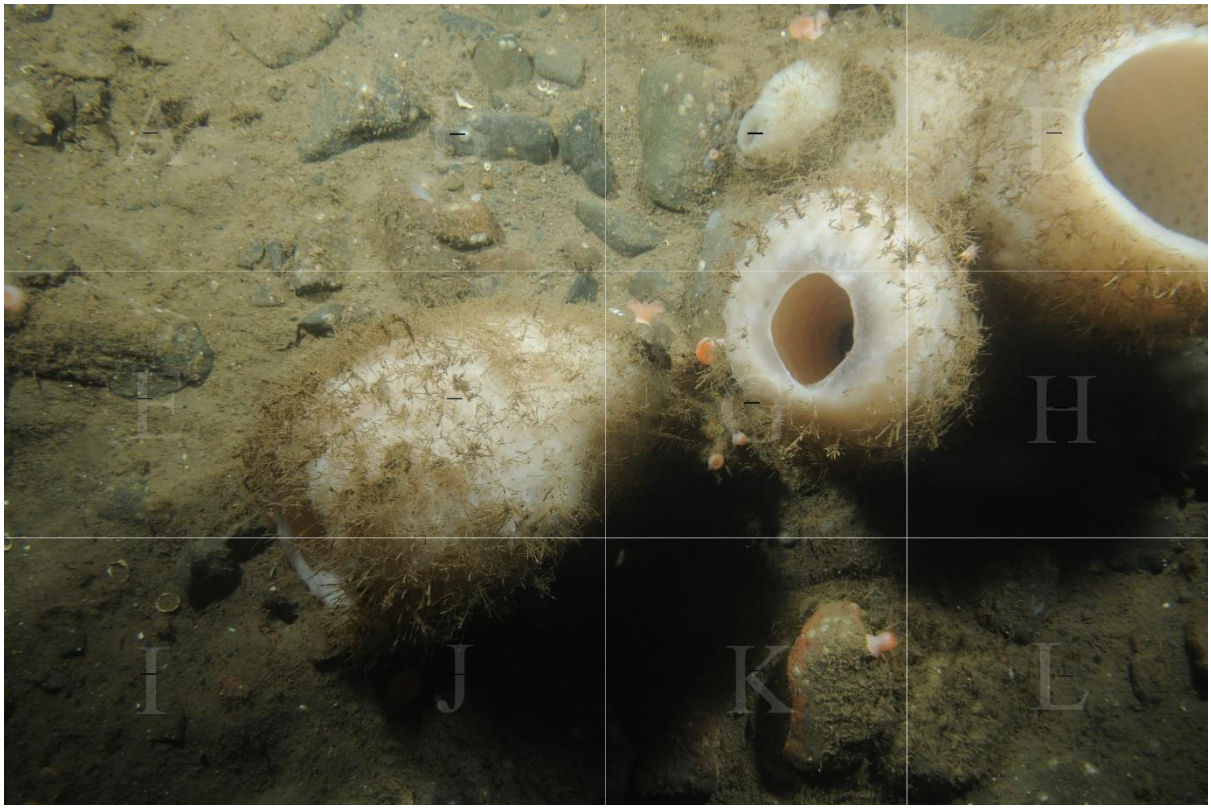

Fig. 2. Grid cells overlain image DSC-2011-06-09 1918412.JPG from CON 20 using batch processing in Adobe Photoshop CS2. Note the black, 1 cm scalebars in the centre of each grid cell.

To prevent annotation bias within transects, the images within transects were analysed randomly. Randomisation of images was achieved by using the "rand()" function followed by the sort command in Excel. The generated sequence of numbers was placed adjacent to the list of images and sorted by increasing order. Features within Photoshop such as the "sharpen", "sharpen more" tools, the manipulation of brightness and contrast, and the marking of certain epibenthic megafauna using the paint brush tool (i.e. to accurately quantify organisms), were also used. Images were analysed alphabetically (A-L) using a constant zoom of 100% in Photoshop to ensure consistency. Epibenthic megafauna were defined as motile and sessile organisms ≥ 1 cm, living on or near the seafloor. Organisms were always recorded in the first cell in which they appeared. Organisms that met these criteria were counted and identified to the lowest possible taxonomic level; however, due to the nature of *in situ* benthic transect images, fine-scale features used to identify different epibenthic megafauna to species level were often too blurry to aid in the identification process, ultimately resulting in assignments to higher taxonomic levels. Morphotype designations were given to megafauna that could not be identified to the species-level such as Porifera (P.) sp. 1 and Asteroidea (C.) sp. 1, with the letter in parentheses denoting the taxonomic level: P, phylum; C, class, O, order, F, family; and, G, genus. The "spp." classification was used to indicate that several species could be present. Epibenthic megafauna that could not be placed at even the Phylum level, were designated as "Unidentified", and were separated by features such as morphology, colour and dimensions. "Unidentified" was used as a separate category in the database (for categorical purposes only, see Fig. 4). All labelling was conducted chronologically except when similar taxa were also found in Beazley and Kenchington's technical report (2015), in these instances, descriptions and labelling were kept as similar as possible. Biogenic structures, including shell hash, burrows, casings, filaments, mounds, spicule mats, tracks and tubes, were also recorded; however, mounds and burrows were recorded on a presence or absence basis per cell, whilst the other biogenic structures were recorded in the same manner as the epibenthic megafauna, i.e. individually. Any observed *Vazella pourtalesii* were recorded in the exact same manner as other epibenthic megafauna, including the abundance per grid cell; furthermore, *Vazella pourtalesii* specimens were separated in three subcategories: live (not sediment-covered, morphologically intact and upright), damaged (morphologically damaged, e.g. flattened or torn) and dead, *Vazella pourtalesii* (sediment-covered, often deformed). These entries were labelled as "Vazella pourtalesi_live", "Vazella pourtalesi_damage" and Vazella pourtalesi_dead in the electronic database. All first-level identification was conducted using three photo books (i. Annelida - Cnidaria, ii. Ctenophora – Porifera and iii. Unidentified) that contained descriptions and photos for reference of the respective taxa, for consistency. If a new taxon was discovered it was referenced and added to the appropriate

photo book for future reference. All changes made to the photo books and database were logged in an Excel spreadsheet, “Photobook changes”, which functioned as a changelog. The changelog gave information on the respective phyla and taxa modified, the change(s) made, the photo and grid cell of change(s), the date, and, a comment section for further information pertaining to the change(s).

All epibenthic megafauna, biogenic structures and the abundances of respective taxa were recorded in a customised form in Microsoft Access (Access 2016), created by Robert Benjamin (DFO), and previously used in several studies such as Korabik (2016), and Beazley and Kenchington (2015) (Fig. 3). All data was recorded physically prior to copying it into the electronic databases. Image metadata including CONs and photo file names were imported into the database using the “Import Photo Data” tab (see Fig. 3), prior to the analyses. The image metadata was stored in a separate table “Photo” (Fig. 3), and the metadata was queried when transects and images were selected for analyses. An extensive description of the database can be found in the Appendix (A1).

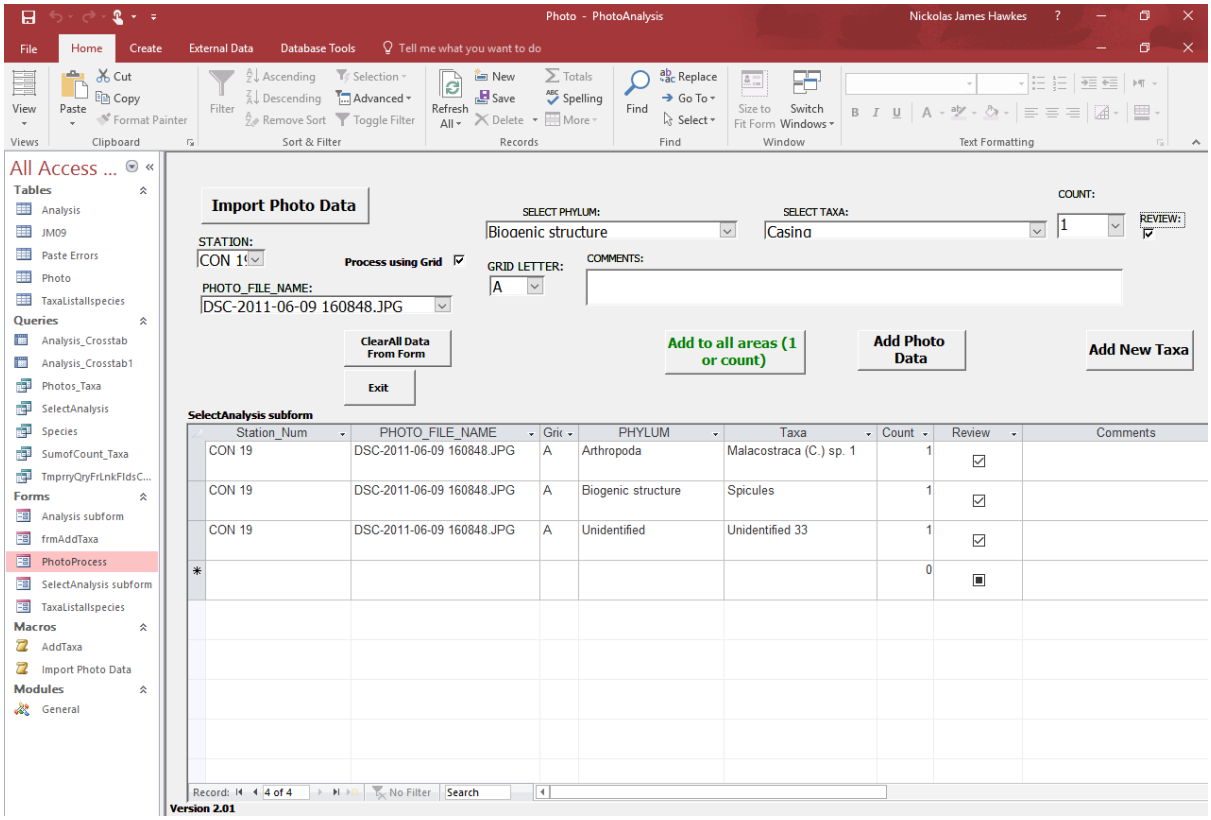

Fig. 3. The photo form where all epibenthic megafauna, biogenic structures and abundance data were recorded. The highlighted tab to the left (in pink) displays this window, the “PhotoProcess” form. This screenshot shows an example entry of a biogenic structure, “Casing”, with an abundance of 1 in grid letter A being added to the database in CON 19, photo DSC-2011-06-09 160848.JPG. Selecting the “Add Photo Data” tab would successfully add the respective entry to the table displayed above. Note the important tables on the left-hand side: “Analysis”, the operative database; “Photo”, a table with all of the image metadata; and, “TaxaListallspecies”, a table of all the observed taxa from the images (a catalogue of all the recorded species).

Adding a new taxa to the Microsoft Access database was achieved by selecting the “Add New Taxa” tab in the photo form (Fig. 6), this brought up a new form, listed as “frmAddTaxa” (Fig. 4). Selecting the arrow at the bottom of the window (highlighted) would create a blank new entry where one would enter all the taxonomical information available (Fig. 4.), with particular emphasis on the correct designated label in “Taxa:”, and correct phylum in “Phylum:”, as these were queried from the “TaxaListallspecies” table to the photo form. The “TaxaListallspecies” table functioned as an ever-changing catalogue of all the different recorded taxa.

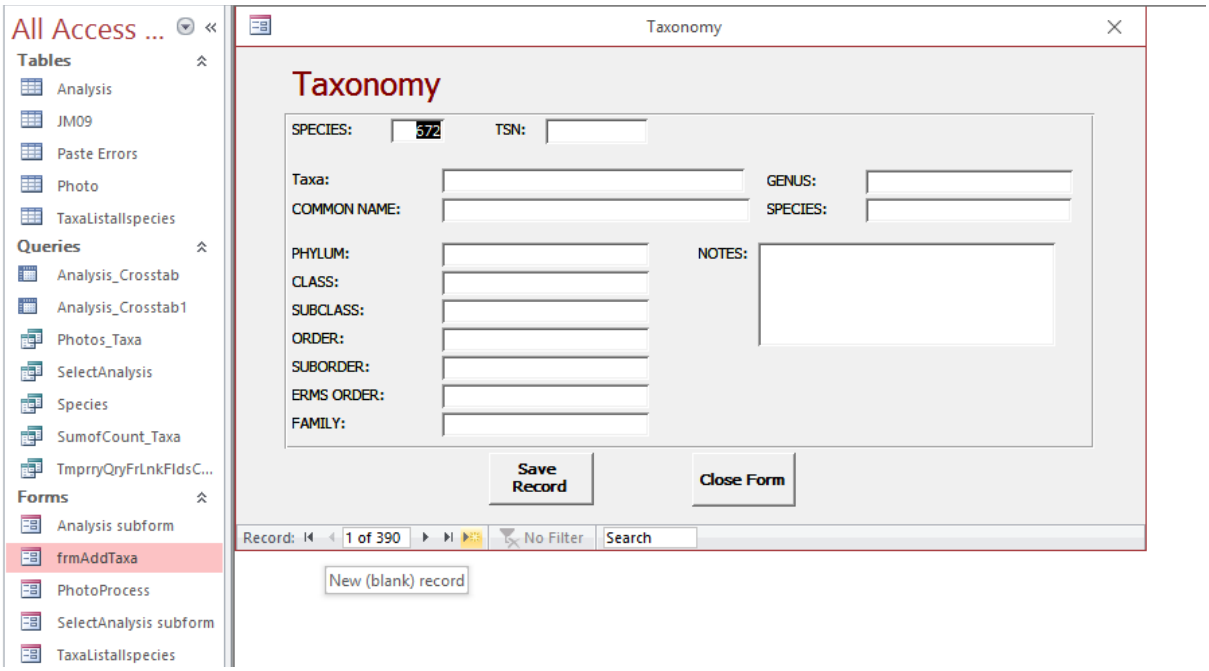

Fig. 4. Mock-example of a taxa being added to the database, Unidentified 384 of the Unidentified “phylum”. The highlighted field on the left in pink under “Forms”, displays this “Taxonomy” form. Upon hitting “Save Record” this data is stored in the “TaxaListallspecies” table which is then queried to the photo process form, allowing it to be selected in the dropdown menus within it. The highlighted arrow in yellow (“New (blank) record”) must be selected prior to saving the record, as failure to do so would result in the failure of recording a new species or morphotype.

Effect of Vazella pourtalesii

The presence or absence and the condition of *Vazella pourtalesii*, as well as the date these data were collected on, per photo (not grid cell), were recorded binarily (yes or no) in an Excel spreadsheet. Both of the factors were later used in final analyses. Five categories pertaining to composition were initially used in the spreadsheet: live, dead, damaged, mixed (i.e. combinations of live, dead or damaged *Vazella pourtalesii* occurring within the same photo) and absent. Images with only damaged *Vazella pourtalesii* were not used in the final analyses due to the small sample size (n = 7).

Effect of substrate

The effect of substrate on the associated biodiversity was also assessed. All substrate data were collected from the same set of benthic images as the epibenthic megafauna data. The open source photo-editing software, GIMP (v. 2.8.22), was used to create transparent layers, labelled as "Area" in GIMP, overlain the image layer. All rocks above 1 cm in images were outlined using the free select tool and filled using the bucket fill tool, with pure black (#000000) as the designated colour. Pixels were counted in a histogram with the "value" channel selected and the "Area" layer selected (to ensure the correct layer was analysed). The pixel counts were recorded and the percentage coverage was calculated by dividing pixel counts with the total pixel count (constant, 12,212,224) and multiplying this value with 100. The quantity of rocks per photo and the type of coverage were also recorded. Four distinct categories were created based on the types of coverage: (i) "sediment-covered" if more than 90% of the coverage of hard substrate was sediment-covered; (ii) "clear", if more than 80% of the surface of hard substrate was visible (including coverage of encrusting poriferans and cnidarians etc.); (iii) "mixed", if the percentage coverage fell under the limits set by the clear and mixed categories; and, (iv) "soft", if no hard substrate was found. Following completion of analyses of hard substrate, photos were saved in GIMP as "x_substrate.xcf", where x would be substituted with the original name of the photo file. All substrate and epibenthic megafauna data were reviewed prior to the final data preparations and analyses.

Data preparation and analyses

The high number of rare taxa would have potentially confounded the final analyses and therefore, a data reduction scheme was used to focus on more abundant and reliably sampled taxa. Two datasets including taxa contributing ≥ 0.5% or ≥ 1% of the total abundance in any one transect were used for the final analyses (≥ 1% analyses can be found in the appendix (Table C2 and Table D2). This was achieved by exporting two queries of the Microsoft Access database into Excel, calculating taxa abundances per transect, removing taxa below the designated percentage threshold and standardising the remaining taxa count data to a 1 m^2 basis (i.e. by dividing the abundance of an organism with the average photo area, 0.401274317 m^2). Due to the high abundances (e.g. 91.75% of the total abundance in CON 21) of *Meganyctiphanes norvegica*, and the fact that it frequently occurred far from the seafloor, this species was not included in the final GLMs and GLMMs in this thesis, as the high abundances also altered the selection of taxa, and therefore, the species-abundance matrices: however, SIMPER and ANOSIM analyses using taxa contributing 0.5% or more of total abundance in any one transect, with the inclusion of this taxon, can be found in the Appendix (Table C3 and Table D3).

Species accumulation curves

Species accumulation curves were generated to ensure that the biodiversity was adequately sampled within each transect and to ensure the reliability of the collected data for the following analyses. Data for the species accumulation curves for each transect were calculated in PRIMER 6 v. 6.1.18.0 (PRIMER-E Ltd., UK), permuted 999 times, and averaged. All the figures and data generated, and the analyses conducted in Primer used the same software version. The final species accumulation curves for each transect were created in Excel to add error bars using the standard deviation (calculated in PRIMER) for each averaged point of the species-accumulation curves. The ANOSIM routine in PRIMER was used to test for differences between transects (i.e. a global test) and subsequently identify which transects were significantly different to each other in pair-wise comparisons. The ANOSIM routines used Bray-Curtis dissimilarity matrices based on log-transformed (log(x+1)) and standardised, count data. Non-metric multi-dimensional scaling (MDS) of Bray-Curtis similarity measures, using Kruskal fit scheme 1, were used to visually examine the potential differences of samples between transects, in PRIMER (25 restarts). Differences between transects were further examined by using the DIVERSE routine in PRIMER to calculate the species richness, total abundance, Shannon diversity (H', base e) and Pielou's evenness *J*' of each sample. All biodiversity indices calculated using the DIVERSE routine in PRIMER used the standardised count data from the species-abundance matrices. The same biodiversity indices were later used in the analyses pertaining to both hypotheses. After failing to meet the assumptions of equal variances (Levene's test) and normality of residuals (Shapiro-Wilk test), non-parametric Kruskal-Wallis tests were used to analyse the transects. Following rejection of the null hypothesis, pair-wise differences between transects were analysed using Dunn's tests with Bonferroni-adjusted p-values in SPSS (v. 25.0.0.0). The more powerful Conover-Iman test (Conover & Iman, 1979) was considered; however, the cumulative distribution functions crossed each other in most instances, violating this test's main assumption.

Influence of Vazella pourtalesii on epibenthic megafauna

Differences in the megafaunal community composition in relation to (i) the presence or absence of *Vazella pourtalesii*, and, (ii) the condition of *Vazella pourtalesii*, were analysed using the SIMPER and ANOSIM routines in PRIMER 6. All further analyses used standardised data from the species-abundance matrices without *Vazella pourtalesii*. The SIMPER routine lists the percentage contributions of species, in decreasing order, to similarity within levels of a factor, and contrarily, the taxa driving the dissimilarity between levels of a factor. A 70% cut-off was used for all conducted SIMPER routines. Log-transformations of standardised count data were conducted to down-weight the effect of highly abundant taxa in the final community analyses (Clarke & Warwick, 2001). The

routines were conducted in the exact same manner as the transects, but with presence or condition as factors. MDS of Bray-Curtis similarity measures (Kruskal fit scheme 1) were used to visually represent and examine the samples (25 restarts). The DIVERSE routine calculated the biodiversity indices of each sample in the different datasets. Following extraction from PRIMER, data were collated with data from the substrate and *Vazella pourtalesii* condition and presence spreadsheets, and subsequently analysed in R (v. 3.4.0) and SPSS (v. 25.0.0.0).

After failing to meet the assumptions of homoscedasticity and normality of residuals, assessed both quantitatively (Levene's tests and Shapiro-Wilk tests) and visually (histograms of the levels of the factor), a GLMM approach was used to determine the effect of coverage and *Vazella pourtalesii* in predicting patterns in biodiversity whilst controlling for the potential random effect of transects. Two distinct GLMMs were used to test both research hypotheses: (I.) GLMMs with percentage coverage of hard substrate or presence (or absence) of *Vazella pourtalesii* in predicting biodiversity; and, (II.) GLMMs with percentage coverage of hard substrate and the condition (live, dead or mixed) of *Vazella pourtalesii* in prediciting biodiversity. Model selection was conducted in three key steps: step-wise within the GLMMs, selecting the model with the lowest AIC and running step-wise likelihood ratio tests; (ii) comparing these models with equivalent GLMs to evaluate the addition of the random effect (AIC); and (iii), comparing the final models to null models (AIC) and conducting likelihood ratio tests. Model fit and evaluation was conducted using the fixed effects models, as these could be easily evaluated using the autoplot function ("ggfortify" package, R). The final evaluation and diagnostics of models can be found in the appendix (Appendix E). Note that percentage coverage of hard substrate and both presence and condition had to be separated as predictor variables due to the strong association between the variables. Potential differences were examined using a Mann-Whitney U test and Kruskal-Wallis test. Prior to fitting GLMMs, the abundances per sample, in all datasets, were rounded to the nearest integer. GLMMs were initially fit with poisson distributions and log link functions ("lme4" package, R); however, overdispersion was present in almost all models, resulting in GLMMs with negative binomial distributions and log link functions ("MASS" package, R) being fitted for the condition GLMMs. Shannon diversity was converted to binary format after poor model predictions and underdispersion ($\varphi < 0.2$). This was achieved by calculating the medians of indices and denoting values below or above the medians as 0s or 1s, respectively. Dispersion (φ) was tested by dividing the squared sum of residuals by the residual degrees of freedom (*sensu* Zuur *et al*., 2009). Overdispersion or underdispersion existed if φ was greater or less than 1, respectively. Pielou's evenness *J*' was analysed with Mann-Whitney U tests (presence or absence) or Kruskal-Wallis tests (i.e. condition: live, dead or mixed), as GLMMs

and GLMs could not be fitted (high underdispersion). Although the quantity of hard substrate (i.e. number of rocks above 1 cm) was analysed, it was not included as a predictor in the final GLMMs as it was very strongly correlated with percentage coverage of hard substrate (Spearman's rank correlation, $r_s = 0.916$, $p < 0.001$). Finally, the R script of the analyses and plots can be found in a shared folder on my google drive (https://drive.google.com/open?id=0BwVAA1yi_ihYbnhQUjhKLVRqYWs).

Results

Summary

In total, 467 photos were analysed across five transects, covering a total area of 187.5 m^2 (Table 1). A total of 35367 individuals representing 239 different taxa and 18334 biogenic structures of 9 unique morphotypes, were recorded (Table 2). 152 taxa could not be confidently placed in any phyla and constituted 18.7% of the observed biota. The remaining 87 taxa, constituting 81.3% of the observed biota, were placed at the lowest possible taxonomic levels in 10 different phyla, with 6 taxa placed at the family level and 7 taxa placed at the species or genus level. The Arthropoda, Cnidaria and Porifera phlya were the most abundant and diverse, representing 46.3%, 20.0% and 9.3% of the total abundance, and 2.9%, 16% and 35% of the observed taxa, respectively. Ctenophora was the least diverse and abundant phylum and taxa (Ctenophora (P.) sp. 1), representing only a single observation in CON 5. The most abundant taxa were *Meganyctiphanes norvegica*, Unidentified 33, Actinaria (O.) spp., Serpulidae (F.) spp. and Actinaria (O.) sp. 4, representing 44.5, 9.4, 6.3, 4.5 and 4.4% of the total abundance of observed biota, respectively.

Table 2.
Abundance (standardised to 1 m^2) and number of taxa for each phylum observed in the Emerald Basin, across five transects. Numbers in parentheses indicate the percentage of total abundance of observed taxa or the percentage value of number of taxa.

Phylum	Total abundance	Number of taxa
Annelida	1619 (4.6)	2 (0.8)
Arthropoda	16387 (46.3)	7 (2.9)
Bryozoa	107 (0.3)	4 (1.7)
Chordata	127 (0.4)	9 (3.8)
Cnidaria	7050 (20.0)	16 (6.7)
Ctenophora	2 (0.006)	1 (0.4)
Echinodermata	171 (0.5)	8 (3.4)
Mollusca	19 (0.1)	4 (1.7)
Nemertea	12 (0.03)	1 (0.4)
Porifera	3277 (9.3)	35 (14.6)
Unidentified	6596 (18.7)	152 (63.6)
Total	35367	239
Biogenic structures	18334	9

Taxa included in further analyses constituted either ≥ 0.5% or ≥ 1% and of the total abundance in any one transect (Table 3); however, GLMMs, ANOSIMs and SIMPERs analyses of the latter taxa (ii), as well as a dataset including taxa contributing to 0.5% or more in any one transect with the krill

species, *Meganyctiphanes norvegica* included, can be found in the appendix (for reasons explained in detail in the methodology). *Meganyctiphanes norvegica* was the most abundant observed taxa, with an overall abundance of 15699, contributing to 44.4% of the total abundance of all observed taxa. Of the 61 (≥ 0.5%) and 39 taxa (≥ 1%) in the final species-abundance matrices, Actinaria (O.) spp., Unidentified 33, Actinaria (O.) sp. 4 and Serpulidae (F.) spp. were the most abundant taxa overall.

Table 3.
Taxa contributing to 0.5% or more of the total abundance of observed biota in any one transect, standardised to 1 m^2. Percentage values are listed first, followed by standardised counts in parentheses, rounded down to the nearest integer. Respective phyla, taxa and brief descriptions are also included. Letter in parentheses with taxa indicate the taxonomic level of identification, i.e.: P, phylum; C, class; O, order; F, family; and G, genus. Summary tables are marked in bold at end of the table. Mean abundance was calculated by dividing the total unstandardised counts by the total area covered by each respective transect. Taxa between 0.5% and 1% are highlighted light blue. The *Vazella pourtalesii* abundance listed here does not include dead individuals.

Phylum	**Taxa**	**Description**	**CON**				
			18	19	20	21	5
Annelida	Serpulidae (F.) spp.	Calcareous tubes with white plume at the end occasionally visible. Observed on rock or horizontally across soft sediment.	22.4 (191)	9.3 (623)	4.3 (373)	13.1 (176)	7.5 (244)
Arthropoda	Malacostraca (C.) sp. 1	Large eyes and a semi-translucent body. Likely *Meganyctiphanes norvegica* or a species of *Pandalidae*.	0.3 (2)	0.6 (39)	0.1 (4)	0.2 (2)	0 (0)
Arthropoda	Malacostraca (C.) spp.	Malacostracan species that cannot be identified confidently.	0.6 (4)	0.2 (12)	0.5 (42)	3.7 (49)	0.2 (4)
Arthropoda	Pandalidae (F.) spp.	*Pandalidae* species with white legs, translucent body and most often epibenthic.	3.2 (27)	2.4 (156)	2.3 (194)	1.9 (24)	2.2 (72)
Bryozoa	Bryozoa (P.) sp. 1	Erect, fan-shaped dichotomous branching bryozoan. Tan to white in colour.	2.0 (17)	0 (0)	0.4 (37)	2.2 (29)	0 (0)
Chordata	Actinopterygii (C.) sp. 2	Alternating bands of solid and spotted brown. Truncate caudal fin, black at tip. Appears to have two dorsal fins.	0.3 (2)	0 (0)	0 (0)	0.6 (7)	0 (0)
Chordata	Didemnidae (F.) sp. 1	Erect, fan-shaped dichotomous branching bryozoan. Tan to white in colour.	0 (0)	0.5 (34)	0.1 (4)	0.4 (4)	0 (0)
Chordata	Sebastes (G.) spp.	Redfish with alternating bands of dark and light red or pink. Genus *Sebastes.*	0 (0)	0.1 (4)	0 (2)	1.5 (19)	0 (0)
Cnidaria	Actinaria (O.) sp. 4	Column 1 – 2 cm in diameter. Tentacles semi-translucent to light pink and about equal size to cup. May be several species.	0 (0)	9.3 (618)	10.5 (904)	0 (0)	1.5 (49)
Cnidaria	Actinaria (O.) sp. 9	Small column, 1 cm in total width (tentacle to tentacle). Long semi-translucent tentacles. Usually on rock and a few on soft sediment.	0 (0)	0.3 (19)	0.4 (37)	0 (0)	19.2 (625)
Cnidaria	Actinaria (O.) spp.	Taxon includes several species of Actinaria that were difficult to distinguish. Usually small, with various colours, hues and size. Individuals are sometimes found on *Vazella pourtalesii* spicules.	2.3 (19)	7.1 (473)	26.1 (2250)	0.6 (7)	18.0 (585)

Cnidaria	Flabellum (G.) spp.	Most likely *Flabellum angulare* although smaller individuals could be *Flabellum macandrewi* (solitary coral). Thick tentacles from a fleshy body. Tentacles approximately 3 times the body width.	0 (0)	0 (0)	2.3 (194)	0 (0)	0.1 (2)
Cnidaria	*Pachycerianthus borealis*	Large white to pink tube-dwelling anemone. Long, typically banded marginal tentacles often in a biplanar array. Oral tentacles small and often hard to see. Oral tentacles are often slightly darker in colour as well.	0 (0)	0.3 (17)	0.3 (22)	0.6 (7)	0 (0)
Cnidaria	Zoantharia (O.) sp. 1	Colonial zoanthid with long polyps. Column is light orange in colour and smooth. Cup orange to white in colour. Could be several species.	9.9 (84)	2.3 (152)	0.1 (9)	1.1 (14)	0 (0)
Cnidaria	Zoantharia (O.) sp. 2	Colonial zoanthid with sediment-covered polyps. White, medium sized cup and one row of very thin, semi-translucent tentacles. Typically on soft substrate.	8.2 (69)	4.2 (279)	1.0 (87)	0.4 (4)	0 (0)
Cnidaria	Zoantharia (O.) spp.	Likely several species based on different colour and habitat. Cannot be confidently distinguished as either Zoantharia (O.) sp. 1 or 2.	2.9 (24)	2.3 (154)	2.6 (226)	1.5 (19)	0.1 (2)
Echinodermata	Ophiuroidea (C.) sp. 1	Red, unbanded with a small disk relative to arm length. 1.5 – 2 cm. Only found on soft substrate.	0.6 (4)	0 (2)	0 (0)	0.6 (7)	0.1 (0)
Echinodermata	Ophiuroidea (C.) spp.	Buried Ophiuroidea species that are found on soft substrate. Small, 1 cm.	1.5 (12)	0.4 (29)	0.1 (12)	0.2 (2)	0.1 (2)
Porifera	Hymedesmiidae (F.) sp. 1	Blue, cushion and encrusting sponge on rock. Surface covered in large circular pore sieves with raised edges. Some may be in the process of closing or closed.	0 (0)	0.5 (32)	1.8 (159)	2.2 (29)	0.2 (4)
Porifera	Hymedesmiidae (F.) sp. 4	White, cushion and encrusting sponge on rock. Often partially sediment-covered. Surface covered in large circular pore sieves with raised edges.	0 (0)	2.1 (137)	4.1 (356)	1.9 (24)	2.5 (82)
Porifera	Polymastia (G.) spp.	Partially buried, relatively large white papilla. Could be Polymastia (G.) sp. 7 and 2 from Beazley and Kenchington (2015).	0 (0)	0 (2)	0 (0)	2.6 (34)	0 (0)
Porifera	Porifera (P.) sp. 1	Thin, grey-translucent and encrusting sponge. Smooth "dotted" surface.	1.2 (9)	0.6 (42)	0.3 (24)	0.2 (2)	0.6 (19)
Porifera	Porifera (P.) sp. 12	Conulated and grey encrusting sponge. Small oscula sometimes visible.	0 (0)	0.6 (39)	0.1 (9)	0 (0)	0.4 (12)
Porifera	Porifera (P.) sp. 14	Yellow, slightly raised sponge on rock with small oscula. Surface is uneven.	0 (0)	0.1 (9)	0.4 (34)	0.6 (7)	0.7 (22)
Porifera	Porifera (P.) sp. 22	Grey and sheet-like encrusting sponge with small oscula often visible.	0 (0)	1.0 (67)	0.8 (69)	0 (0)	2.3 (74)
Porifera	Porifera (P.) sp. 29	Encrusting sponge that is sediment-covered. Distinguishable from Porifera	0 (0)	0.1 (4)	0.1 (9)	0.6 (7)	0.1 (2)

		(P.) sp. 53 and sp. 5 by large, raised oscula and a relatively even surface.					
Porifera	Porifera (P.) sp. 4	Cloudy white sponge with large, flat oscula seen. Sometimes partially covered in sediment. Could be several species.	3.8 (32)	2.8 (186)	3.3 (289)	1.1 (14)	6.9 (221)
Porifera	Porifera (P.) sp. 43	Grey or off-white cushion, encrusting sponge. Surface appears tuberculate with a few oscula visible. Raised edges.	0.3 (2)	1.0 (69)	0.3 (29)	0.2 (2)	0.9 (29)
Porifera	Porifera (P.) sp. 49	White sponge with branching, cylindrical extensions growing on *Vazella pourtalesii*. Oscula seen dotting the surface.	0 (0)	0 (0)	0 (0)	2.8 (37)	0.1 (2)
Porifera	Porifera (P.) sp. 5	Sediment-covered sponge. Could be Hymedesmiidae (F.) sp. 4. Very thin, sometimes raised oscula.	0.3 (2)	0.1 (7)	0.7 (62)	0 (0)	2.7 (87)
Porifera	Porifera (P.) sp. 51	Encrusting sponge, irregularly shaped and often partially sediment-covered. Spots or lines of white sometimes visible. 1-2 cm with minute oscula. Surface appears wrinkled.	0 (0)	0 (0)	0 (0)	0.9 (12)	0.2 (7)
Porifera	Porifera (P.) sp. 53	Similar to Porifera (P.) sp. 5, but thicker. Sediment-covered, irregular and uneven.	0.6 (4)	0.1 (4)	0.2 (14)	0.6 (7)	0.1 (2)
Porifera	Porifera (P.) sp. 56	Morphologically similar to *Hymedesmiidae* (F.) sp. 1, but bright green in colour. Occasionally sediment-covered.	0 (0)	0.1 (4)	2.1 (179)	3.5 (47)	0.3 (9)
Porifera	Porifera (P.) sp. 8	White semi-translucent sponge with white speckles (tuberculated?). Has small oscula and defined edges.	0 (0)	1.4 (92)	0.7 (57)	0 (0)	0.2 (7)
Porifera	*Vazella pourtalesii*	White, vase-shaped sponge attached to hard substrate. Spicules on the exterior often accumulate flocculent material.	3.5 (29)	6.9 (458)	5.9 (510)	3.9 (52)	4.7 (152)
Unidentified	Unidentified 1	White, sediment-covered, globular organism. Could be a sponge or ascidian.	0.3 (2)	0 (2)	0 (2)	0.6 (7)	0.1 (2)
Unidentified	Unidentified 103	White, oval-shaped and slightly raised organism in sediment or on a rock. Surface can have a slight sheen, could be *Anomia.*	0 (0)	1.1 (72)	0.6 (52)	0.9 (12)	0 (0)
Unidentified	Unidentified 12	Sediment-covered and thin organism. Could be a terebellid worm, 1 – 3 cm.	0.6 (4)	0.5 (34)	4.0 (343)	2.0 (27)	5.4 (174)
Unidentified	Unidentified 120	Banded, long (> 3 cm), tube-shaped organism with a yellowish-brown tuft at the tip. Possibly a zoanthid.	0 (0)	0.1 (4)	0.1 (7)	0.6 (7)	0 (0)
Unidentified	Unidentified 174	Small (1 cm), tubular organism terminating to a bright white tip.	0 (0)	0 (0)	0.1 (7)	0.6 (7)	0 (0)
Unidentified	Unidentified 185	Speckled, encrusting organism on rock. Slightly raised. Potentially a poriferan or Unidentified 103.	0 (0)	0 (0)	0.1 (7)	0.6 (7)	0.1 (2)
Unidentified	Unidentified 19	Grey, encrusting, irregular and uneven organism. Possibly Porifera (P.) sp. 12.	0 (0)	0.7 (47)	0.1 (12)	0 (0)	0.1 (2)

Unidentified	Unidentified 196	Teal, encrusting organism. Uneven surface. Potentially a poriferan. Appears to have oscula.	0 (0)	0 (0)	0 (2)	0.6 (7)	0 (0)
Unidentified	Unidentified 208	White sponge-like organism growing on *V. pourtalesii* (> 2 cm).	0 (0)	0 (0)	0.1 (12)	0.7 (9)	0 (0)
Unidentified	Unidentified 21	Sediment-coloured, with branches from an axial stalk. Ocassionally found on *V. pourtalesii*. Bryozoan?	2.0 (17)	0.6 (37)	0.3 (27)	3.7 (49)	1.2 (37)
Unidentified	Unidentified 22	1 cm tubes found in the spicules of *V. pourtalesii*.	1.7 (14)	2.9 (191)	2.4 (206)	3.5 (47)	1.5 (49)
Unidentified	Unidentified 23	Thin, sediment-coloured, membranous-like organism (> 2 cm).	1.2 (9)	0 (0)	0.1 (4)	0.4 (4)	0 (0)
Unidentified	Unidentified 25	Typically greater than 1.5 cm, thin, sediment-covered organism.	0 (0)	5.9 (393)	1.5 (127)	0.2 (2)	1.1 (34)
Unidentified	Unidentified 250	Beige, colonial (?) tube-like organisms on hard substrate. Possibly zoanthids (1 cm).	0 (0)	0 (0)	0 (0)	0.7 (9)	0 (0)
Unidentified	Unidentified 27	Thin, pale, sediement-covered tubular organism. Possibly *Serpulidae*.	0 (0)	1.0 (69)	0.2 (19)	0.2 (2)	0.4 (12)
Unidentified	Unidentified 276	Encrusting organism on hard substrate. Possibly a poriferan, however, no oscula are visible. Irregular-shaped (1 cm) and similar to Unidentified 209.	0 (0)	0 (0)	0 (0)	1.9 (24)	0.4 (12)
Unidentified	Unidentified 28	Thin, round, speckled encrusting organism with white spots in its centre.	0.3 (2)	0.9 (62)	2.4 (206)	0.9 (12)	1.2 (37)
Unidentified	Unidentified 29	Sediment-covered, light, plate-like organism.	0.6 (4)	0 (0)	0 (0)	0 (0)	0 (0)
Unidentified	Unidentified 30	Sediment-covered, colonial (?) organisms. Possibly zoanthids.	1.2 (9)	0 (0)	0 (0)	0 (0)	0 (0)
Unidentified	Unidentified 33	Tubular organism with a curled tip, typically 1 cm.	23.6 (201)	18.8 (1253)	4.0 (341)	16.9 (226)	6.4 (209)
Unidentified	Unidentified 38	Beige, dome-shaped organism on a rock.	0 (0)	1.0 (64)	0.3 (24)	0 (0)	0.1 (2)
Unidentified	Unidentified 52	Sediment-coloured, elliptical organism on hard substrate. Possibly *Terebratulina*.	0 (0)	1.1 (72)	1.4 (117)	0 (0)	0.3 (9)
Unidentified	Unidentified 61	Long (> 2-3 cm), sediment-covered and thin, tubular organism.	0 (0)	0.6 (42)	0.7 (57)	3.2 (42)	0.7 (22)
Unidentified	Unidentified 71	Sediment-covered tube with a yellow tip. Appears to taper to one end.	0 (0)	0.1 (7)	0 (0)	0.7 (9)	0 (0)
Unidentified	Unidentified 80	White, twisted strands on sediment.	0 (0)	0.1 (4)	1.5 (127)	1.7 (22)	0.2 (7)
Unidentified	Unidentified 87	Sediment-coloured, globular organism with one thin appendage protruding from its ventral side.	0 (0)	0.1 (4)	0.1 (7)	0.6 (7)	0.4 (12)

Transects

CON 20 was the most diverse transect with the highest mean abundance of taxa, total abundance of taxa, number of taxa and number of rare taxa (Table 4). CON 19 and CON 5 were similar in terms of diversity and mean abundance of taxa; however, CON 19 had more than twice the total abundance of taxa. CON 21 had the second highest number of taxa, but had a much lower abundance of species compared to CON 20, 19 and 5. CON 18 had the lowest diversity and abundance of taxa. Percentage

coverage of hard substrate was highest in CON 5, followed by CONs 19 and 20, respectively (Table 4). CON 5 also had the highest quantity of hard substrate, followed by CONs 20 and 19, respectively (Table 4).

Table 4.
Summary information of each transect and the taxa therein (taxa contributing to ≥ 0.5% of the abundance in any one transect). Total abundance of all taxa refers to all observed taxa, without the inclusion of *Meganyctiphanes norvegica* (hence the difference to the value listed in Table 2). Abundances are standardised to 1 m^2 and rounded down to the nearest integer. The mean abundances of taxa per transect were calculated by dividing the unstandardised sum of count data, for the respective transect, by the total estimated area of the respective transect (Table 1). Values listed in parenthesis denote the interquartile range (IQR) of coverage of hard substrate (%) and quantity of hard substrate. The number of photos analysed are also listed in Table 1.

Summary of transects	CON 18	CON 19	CON 20	CON 21	CON 5	All
Mean abundance of taxa	13	36	61	22	36	38
Total abundance of taxa	785	5689	7421	1161	2808	17865
Total abundance of all taxa	824	6210	8119	1290	3097	19542
Number of taxa	26	46	50	48	40	60
Number of rare taxa	16	68	95	45	66	177
Median coverage (%) (IQR)	0.316 (0.155-1.11)	6.74 (0.815-16.5)	6.14 (1.15-17.3)	0.24 (0.053-1.96)	24.6 (13.6-32.5).	3.37 (0.314-15.4).
Median quantity (IQR)	2 (1-6)	8.5 (3-36)	21 (4-43)	2 (1-6)	55 (40.8-80.3)	9 (2-39)
Number of photos	60	156	121	78	52	467

Species-accumulation curves of each transect (Fig. 5) nearly approached their respective asymptotes, indicating that the sampling effort was high enough to give fair representations of the actual epibenthic megafaunal communities and the patterns of biodiversity therein. The levelling off towards an asymptote was clearer in species-accumulation curves of the "1% taxa" (Fig. 5). CON 21 showed the largest deviance between species-accumulation curves of 0.5% (or more) and 1% (or more) taxa.

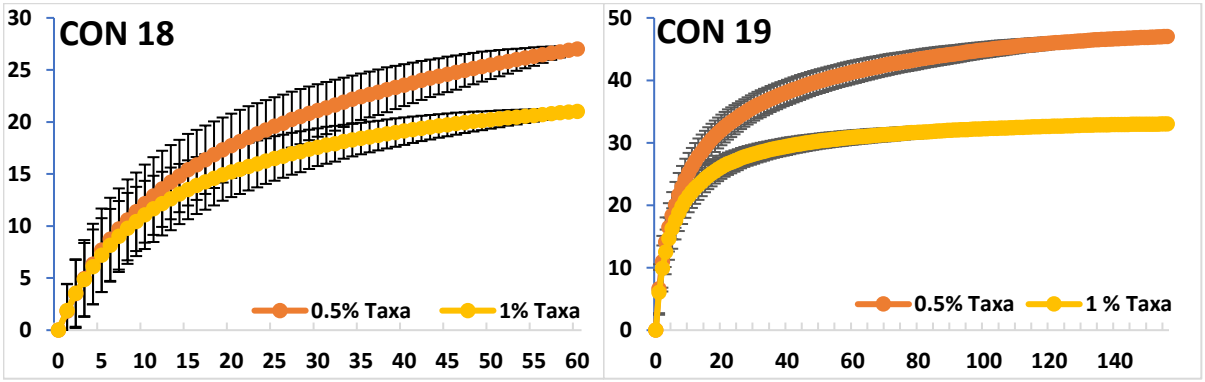

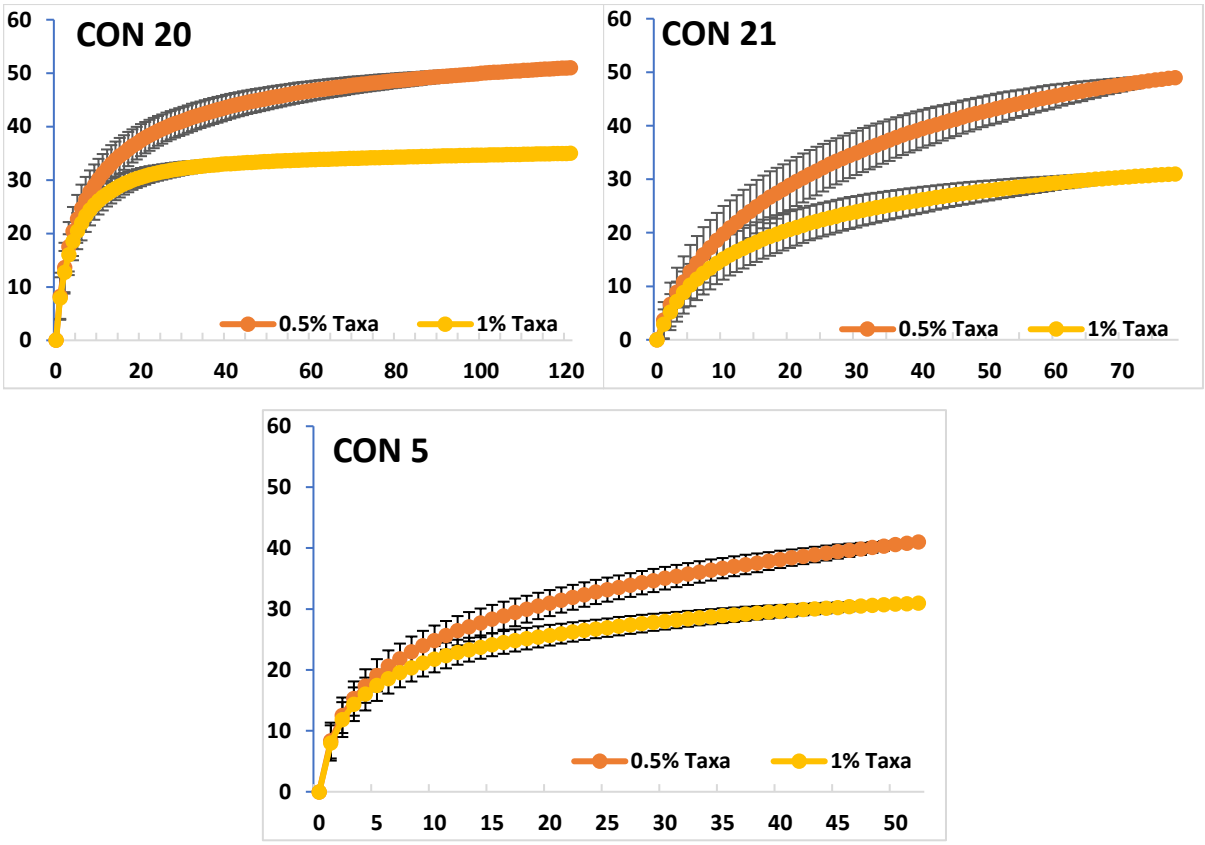

Fig. 5. Species-accumulation curves of each transect with taxa contributing to 0.5% or more, and, 1% or more, of the total abundance in any one transect. Orange and yellow denote 0.5% or 1% taxa, respectively. The error bars indicate the standard deviation. The distance between tick marks on the x-axes of all plots is 5.

Kruskal-Wallis H tests, adjusted for ties, were conducted to test for differences in the species richness, abundance, Shannon diversity (H') and Pielou's evenness *J*' between transects (species richness: $\chi^2(4) = 150.240$, $p < 0.0001$, $n = 467$; abundance: $\chi^2(4) = 165.961$, $p < 0.0001$, $n = 467$; Pielou's evenness *J*': $\chi^2(4) = 51.681$, $p < 0.0001$, $n = 390$; Shannon diversity (H'): $\chi^2(4) = 131.477$, $p < 0.0001$, $n = 467$). Following rejections of the null hypotheses of Kruskal-Wallis H tests; Dunn's tests (Dunn, 1964), with Bonferroni-corrected p-values, were performed to test which transects were different to each other. A summary of the results of these tests, as well as box plots of the biodiversity indices can be found in the appendix (B1 and B2, respectively). CONs 20 and 21, 21 and 19, and, 5 and 21, shared statistically significant differences in all biodiversity indices (Table B1). A one-way ANOSIM was also conducted to test if the composition of the epibenthic megafaunal communities within transects were different to each other. The composition of megafaunal communities among transects were significantly different to each other (ANOSIM, global $R = 0.305$, $p < 0.001$, 999 permutations). All transects were significant to each other ($p < 0.002$), with the largest difference found between CON 18 and 20 ($R = 0.528$, Table B3). The corresponding SIMPER analysis revealed low average similarity of 6.17% and 16.27% in CON 18 and 21, respectively (Table B4) The MDS showed clear separation of CON 18 from the other transects (Fig. 6), whilst most of the other

samples were confined to a relatively small area of the two-dimensional space. A Kruskal-Wallis H test, adjusted for ties, was conducted to test for differences between coverage (%) of hard substrate between transects. There were statistically significant differences in the mean rank sums of hard substrate between transects (Kruskal-Wallis H test: $\chi^2(4) = 147.48$, $p < 0.001$, $n = 467$). Following the rejection of the null hypothesis of the Kruskal-Wallis H test; Dunn's tests, with Bonferroni-corrected p-values, were performed to test which transects were different to each other. All pair-wise tests except the pair-wise comparisons of CON 21 and 18, and, CON 19 and 20, were statistically significant ($p < 0.001$, Table B5). Percentage of hard coverage between transects are visualised by box plots in the appendix (Fig. B6).

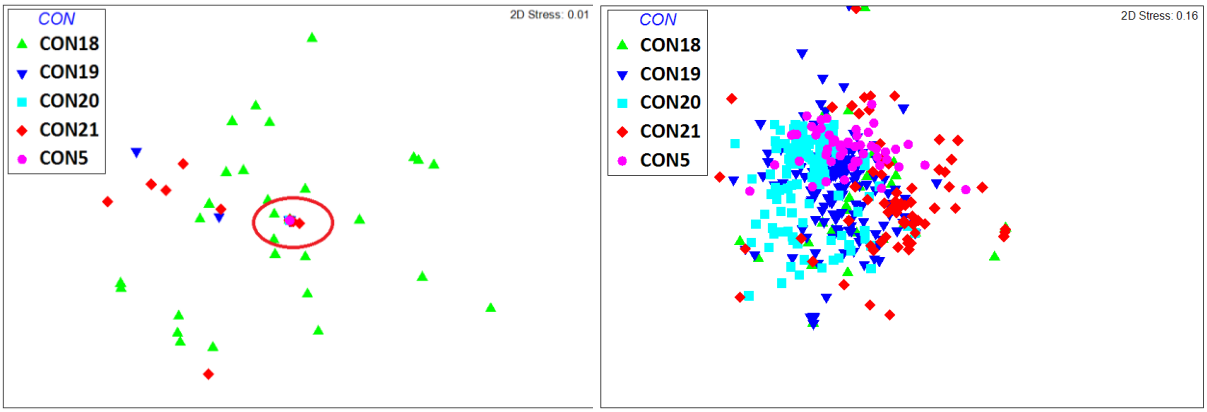

Fig. 6. MDS based on the Bray-Curtis similarity matrix calculated on the log(x+1) species-abundance matrix. Left MDS is the original (no zoom) with low stress (0.01). MDS on the right is a more in-depth representation of the cluster outlined (GIMP) on the left, and was generated using the "subset MDS" function in PRIMER (note the higher stress of 0.16).

Influence of *Vazella pourtalesii* and the substrate on the epibenthic megafaunal communities

Vazella pourtalesii was present in almost two thirds of the photos (Table 5), found in all transects and was the 6th most abundant taxa overall (Table 3). Dead *Vazella pourtalesii* contributed to the majority of the total *Vazella pourtalesii* abundance, followed by live and damaged individuals, respectively (Fig. 7, Table 5).

Table 5.
The observed *Vazella pourtalesii* in each transect. "Present" and "absent" refer to photos with or without *Vazella pourtalesii*, respectively. Live, dead and damaged columns are the standardised (1 m^2) abundances rounded down to the nearest integer. Sum refers to the sum of values in each respective column. Total column is the sum standardised abundances of live, dead and damaged *Vazella pourtalesii* rounded down to nearest integer, within and across transects. Note that the total values differ from the sum of live, dead and damaged *Vazella pourtalesii* listed here, as raw abundance data were used (subsequently rounded down to nearest integer).

CON	Present	Absent	Live	Dead	Damaged	Total
CON 18	16	44	19	161	9	191
CON 19	115	41	428	2751	29	3209
CON 20	96	25	473	1891	37	2402
CON 21	20	58	49	87	2	139
CON 5	50	2	129	2183	22	2335
Sum	297	170	1098	7073	102	8278

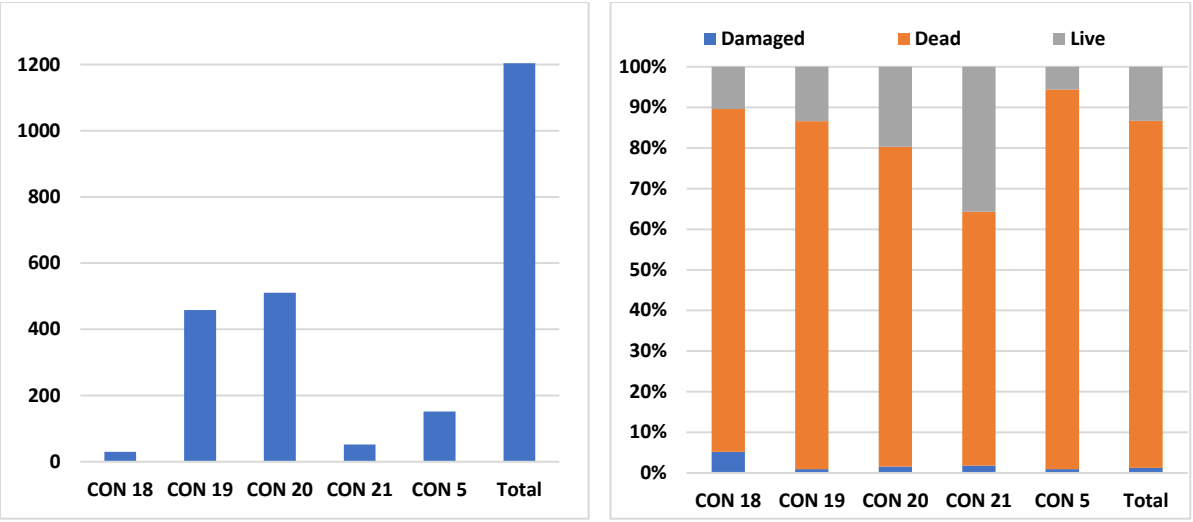

Fig. 7. Bar graph on the left depicts the standardised abundance ($\frac{count}{1\ m^2}$) of *Vazella pourtalesii* (summarisation of live and damaged *V. pourtalesii*) in each transect. These are equivalent to the abundance values of *Vazella pourtalesii* listed in parentheses in Table 3. Bar graph on the right depicts the relative contribution of different conditions of *Vazella pourtalesii* to the total *Vazella pourtalesii* abundance, among and across all transects (total).

The epibenthic megafaunal composition was significantly different between areas with and without *Vazella pourtalesii* present (ANOSIM, global R = 0.347, p < 0.001, n = 467, 999 permutations). A high level of distinction between areas with and without the presence of *Vazella pourtalesii* was indicated by a high average SIMPER dissimilarity of 87.53% (Table 6.). The low average similarity of areas absent of *V. pourtalesii* was also only 11.15%. Differences in megafaunal composition between these areas were also clearly represented by MDS (Fig. 8). Areas without *Vazella pourtalesii* present occupied a much larger area of the two-dimensional space, whilst areas with *Vazella pourtalesii* present were tightly clustered in a much smaller area (Fig. 8). Using a 70% cut off for cumulative contributions of taxa to average dissimilarity, only one taxa, Zoantharia (O.) sp. 2, had a higher average abundance in areas without *Vazella pourtalesii* present (Table 6). Of the 60 taxa contributing to 100% of the average dissimilarity between areas with and without *Vazella pourtalesii*, 80% of taxa (log-transformed species-abundance matrix) had higher average abundances in areas with *Vazella pourtalesii* (Table C1). Results of the SIMPER (70% cut off) and ANOSIM analyses of taxa contributing to 1% or more in any one transect, and taxa contributing to 0.5% or more of the total abundance in any one transect, including *Meganyctiphanes norvegica*, can be found in the appendix (Tables C2 and C3, respectively). Of the species contributing to 70% of the dissimilarity between areas with and without *V. pourtalesii* (Table 6), 9 out of the 14 species were associated with hard bottoms: the Actinarians, Actinaria (O.) spp., Actinaria (O.) sp. 4 and 9; encrusting polychaete, Serpulidae (F.) spp.; encrusting sponges, Porifera (P.) sp. 4 and Hymedesmiidae (F.) sp. 4; the encrusting, shell-like organism, Unidentified 28; and the tubular organism, Unidentified 25. Unidentified 33 was most

often observed in close vicinity of *V. pourtalesii*, and Unidentified 22 was an epifaunal tubular organism uniquely found on *V. pourtalesii.*

Table 6. Taxa contributing up to approximately 70% of the average dissimilarity between areas with and without *Vazella pourtalesii* present. Average abundances are based on the scale of the input data sheet (i.e. the log-transformed species-abundance matrix). Average dissimilarity is the contribution of the respective taxa to the total average dissimilarity (i.e. 87.53%). Multiplying the respective fractions by 100 gives the contribution values in percent listed below. The cumulative contribution in percent is simply a step-wise summarisation of the contribution (%) values.

Taxa	Average abundance – *V. pourtalesii* present	Average abundance – *V. pourtalesii* Absent	Average dissimilarity	Standard deviation	Contribution (%)	Cumulative contribution (%)
Unidentified 33	1.43	0.7	9.47	0.84	10.82	10.82
Actinaria (O.) spp.	1.59	0.3	8.88	1.08	10.14	20.96
Serpulidae (F.) spp.	1.05	0.3	6.64	0.89	7.59	28.55
Actinaria (O.) sp. 4	1.02	0.18	5.63	0.85	6.43	34.98
Pandalidae (F.) spp.	0.55	0.26	4.15	0.69	4.74	39.72
Porifera (P.) sp. 4	0.7	0.07	3.8	0.67	4.34	44.06
Unidentified 12	0.58	0.15	3.77	0.67	4.3	48.37
Zoantharia (O.) sp. 2	0.28	0.33	3.74	0.51	4.27	52.64
Zoantharia (O.) spp.	0.28	0.22	3.14	0.43	3.59	56.23
Unidentified 25	0.48	0.12	2.96	0.58	3.39	59.61
Unidentified 22	0.51	0	2.93	0.53	3.34	62.96
Actinaria (O.) sp. 9	0.46	0.05	2.74	0.47	3.13	66.09
Hymedesmiidae (F.) sp. 4	0.5	0.03	2.34	0.56	2.68	68.77
Unidentified 28	0.34	0.06	1.74	0.53	1.99	70.76

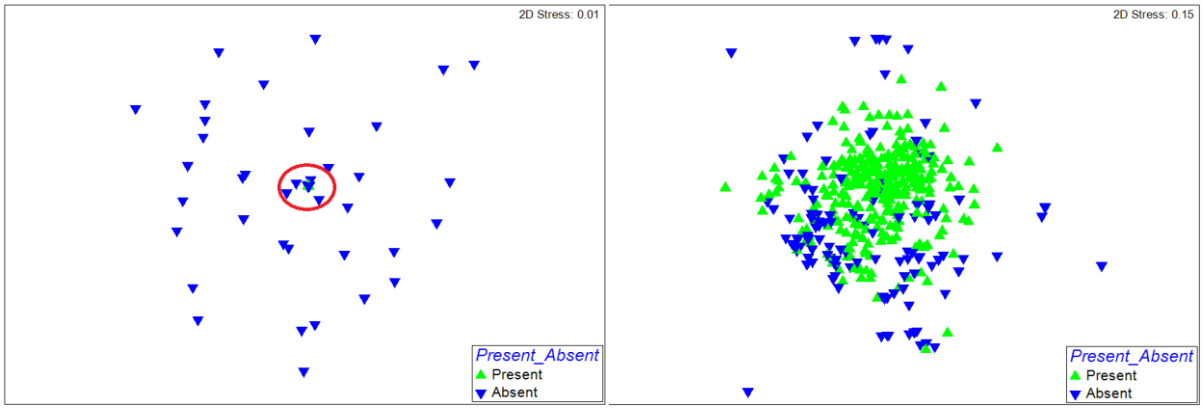

Fig. 8. MDS based on the Bray-Curtis similarity matrix calculated on the log(x+1) species-abundance matrix. Left MDS is the original (no zoom) with low stress (0.01). MDS on the right was generated using the "subset MDS" function in PRIMER (note the higher stress, 0.15), and represents a more in-depth view of the cluster outlined with a red ellipse using GIMP, in the MDS on the left. Photos with and without *Vazella pourtalesii* are depicted by green and blue triangles, respectively.

Coverage was a significant predictor in all final GLMMs with species richness, abundance and Shannon diversity (H') as the individual response variables ($p < 0.001$; Table 7). The first- and second-order terms in all final GLMMs using coverage as a predictor were positive and negative (Table 7), respectively, resulting in the predicted quadratic curves opening downwards. *V. pourtalesii* was a

statistically significant predictor of species richness, abundance, and Shannon diversity (H') ($p < 0.001$) in all three of the final GLMMs; and furthermore, the predicted and observed means of species richness and abundance were higher in areas with *V. pourtalesii* present (Fig. 9). Differences in Pielou evenness *J'* between areas with and without *V. pourtalesii* were tested using a Mann-Whitney U test with continuity correction after GLMMs (with quasi-poisson distributions and log link functions) failed to account for severe underdispersion ($\varphi \approx 0.016$) and gave poor predictions. The final model selections of GLMMs with coverage (%) and presence (or absence) as individual separate predictors can be found in the appendix (Tables C5 and C6, respectively). Pielou evenness *J'* was significantly lower in areas with *V. pourtalesii* present (median, IQR: 0.88, 0.79-0.92; $n_1 = 290$) compared to areas absent (median, IQR: 0.92, 0.87-1, $n_2 = 97$) of *V. pourtalesii* (Mann-Whitney $U = 19934$, $p < 0.001$, two-tailed; Fig. 9).

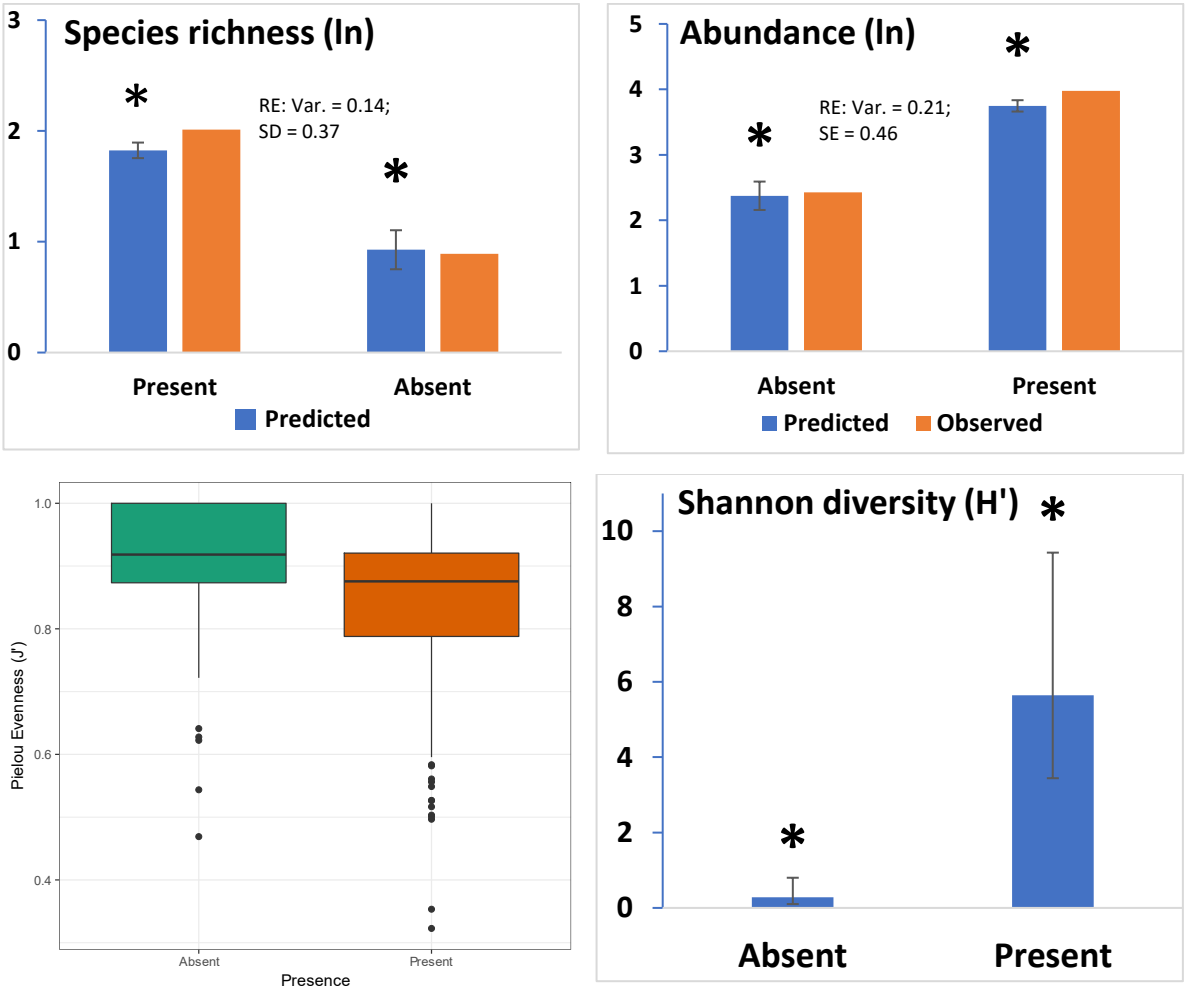

Fig. 9. Relationship between areas with or without *V. pourtalesii* present and the biodiversity indices. The observed and predicted values are compared to assess the validity of the predictions from the GLMMs. The predicted species richness, abundance and Shannon diversity (H') were extracted from the GLMMs in R. Shannon diversity (H') values are odds ratios with 95% CIs. Box plots of Pielou evenness *J'* show the medians and IQRs of areas with ("present") and without ("absent"), *V. pourtalesii*. Asterisks indicate significant differences. "RE" refers to the random effect with "Var." and "SD denoting the variance and standard deviation of the random effect.

Table 7. Summary of the final GLMMs with coverage (%) as a predictor of the respective biodiversity indices: species richness, abundance and Shannon (H') diversity (n = 467 for all models). "Coeff." is the shortened term for the coefficients of the GLMMs and "SE" the standard error. The random effects of each respective model are listed in the table, along with the variance and standard deviation of the respective random effects. The link in parentheses denotes the link function used.

Fixed effects	β	SE	*Z* score	*P*-value	Random effect	Var.	SD
Species richness (negative binomial distribution, link = log)							
Intercept	1.46	0.14	10.36	$< 2.0 \times 10^{(-16)}$	CON (5 transects)	0.010	0.31
Cov.	10.19	0.44	23.30	$< 2.0 \times 10^{(-16)}$			
$Cov.^2$	-3.59	0.39	-9.11	$< 2.0 \times 10^{(-16)}$			
Abundance (negative binomial distribution, link = log)							
Intercept	3.20	0.16	19.82	$< 2.0 \times 10^{(-16)}$	CON (5 transects)	0.12	0.35
Cov.	15.02	0.90	16.69	$< 2.0 \times 10^{(-16)}$			
$Cov.^2$	-5.32	0.69	-7.68	$< 1.6 \times 10^{(-14)}$			
Shannon Diversity (binomial distribution, link = logit)							
Intercept	0.056	0.30	0.19	0.85	CON (5 transects)	0.31	0.56
Cov.	39.78	4.46	8.92	$< 2.0 \times 10^{(-16)}$			
$Cov.^2$	-13.39	3.48	-3.84	< 0.0001			

The epibenthic megafaunal compositions were significantly different between the three different conditions (live, mixed and dead) of *V. pourtalesii* (ANOSIM, global $R = 0.101$, $p < 0.001$, n = 290, 999 permutations); however, pair-wise tests indicated that only the differences between dead and live (ANOSIM, $R = 0.111$, $p < 0.001$, n = 290, 999 permutations) and, dead and mixed (ANOSIM, $R = 0.157$, $p < 0.001$, n = 290, 999 permutations) areas, were significant. MDS (Fig. D1) was used to visualise the relationships of the samples; however, the high stress (0.24) and poor fit, reflected by a Shepard diagram (generated in PRIMER, Fig. D1) indicated that the 2D MDS was a poor representation of the samples. Differences between areas with only live or mixed *V. pourtalesii* were small and not statistically significant (ANOSIM, $R = 0.02$, $p = 0.214$, n = 290, 999 permutations). The average SIMPER dissimilarities between the different conditions were high: 76.54%, 75.57% and 70.72%, for the dead and live, dead and mixed, and, live and mixed samples, respectively (Table 7). Results of the SIMPER (70% cut off) and ANOSIM analyses of taxa contributing to ≥ 1% (without *Meganyctiphanes norvegica*) and taxa contributing to ≥ 0.5% of the total abundance in any one transect, including *Meganyctiphanes norvegica*, can be found in the appendix (Tables D2 and D3, respectively).

Table 7.
Following rejection of the null hypothesis of the one-way ANOSIM, pair-wise differences were further tested with new ANOSIMs, and the SIMPER routine was used to identify the taxa driving the differences. "Groups compared" refers to the respective pair-wise comparisons: DL refers to the comparison between samples with dead and live *V. pourtalesii*; DM refers to the comparison between samples with dead and mixed *V. pourtalesii*; and, LM refers to the comparison between samples with live and mixed *V. pourtalesii*. The average abundances of "Condition 1" and "Condition 2" refers to the respective order the groups listed in "Groups compared". Average abundances are based on the scale of the input data sheet (i.e. the log-transformed species-abundance matrix). Average dissimilarity is the contribution of the respective taxa to the respective total average dissimilarities (DL = 76.54%, DM = 75.57% and ML = 70.72%). Multiplying the respective fractions by 100 gives the contribution values in percent listed below. The cumulative contribution in percent is simply a step-wise summarisation of the contribution (%) values for the respective groups compared. DM field is only highlighted as a visual aid to separate the pair-wise comparisons.

Groups compared	Taxa	Average abundance – Condition 1	Average abundance – Condition 2	Average dissimilarity	Standard deviation	Contribution (%)	Cumulative contribution (%)
DL	Actinaria (O.) spp.	0.93	1.91	7.64	1.2	9.98	9.98
DL	Unidentified 33	1.66	1.13	6.23	1.02	8.14	18.12
DL	Serpulidae (F.) spp.	0.9	0.97	5.51	0.99	7.19	25.31
DL	Actinaria (O.) sp. 4	0.51	1.25	5.46	1.02	7.13	32.44
DL	Unidentified 12	0.55	0.54	3.63	0.85	4.74	37.18
DL	Porifera (P.) sp. 4	0.53	0.68	3.59	0.87	4.69	41.87
DL	Unidentified 25	0.45	0.64	3.58	0.8	4.68	46.55
DL	Unidentified 22	0	0.76	3.51	0.75	4.59	51.13
DL	Pandalidae (F.) spp.	0.52	0.48	3.04	0.83	3.98	55.11
DL	Actinaria (O.) sp. 9	0.63	0.2	3.03	0.64	3.96	59.07
DL	Zoantharia (O.) sp. 2	0.41	0.29	2.98	0.57	3.89	62.96
DL	Zoantharia (O.) spp.	0.32	0.3	2.56	0.55	3.35	66.31
DL	Hymedesmiidae (F.) sp. 4	0.25	0.42	2.13	0.62	2.79	69.1
DL	Unidentified 28	0.18	0.34	1.67	0.65	2.19	71.29
DM	Actinaria (O.) spp.	0.93	1.84	6.73	1.21	8.9	8.9
DM	Unidentified 33	1.66	1.45	5.7	0.98	7.55	16.45
DM	Serpulidae (F.) spp.	0.9	1.17	5.08	1.06	6.72	23.17
DM	Actinaria (O.) sp. 4	0.51	1.2	4.76	1.03	6.3	29.47
DM	Porifera (P.) sp. 4	0.53	0.83	3.64	0.9	4.81	34.28
DM	Actinaria (O.) sp. 9	0.63	0.51	3.54	0.72	4.68	38.97
DM	Unidentified 12	0.55	0.62	3.32	0.85	4.39	43.36
DM	Pandalidae (F.) spp.	0.52	0.6	3.08	0.84	4.07	47.43
DM	Hymedesmiidae (F.) sp. 4	0.25	0.71	2.77	0.78	3.66	51.09
DM	Unidentified 25	0.45	0.42	2.67	0.71	3.53	54.63
DM	Unidentified 22	0	0.68	2.67	0.65	3.53	58.15
DM	Zoantharia (O.) sp. 2	0.41	0.17	2.34	0.57	3.1	61.25
DM	Zoantharia (O.) spp.	0.32	0.24	2.18	0.5	2.88	64.13
DM	Unidentified 28	0.18	0.44	1.82	0.63	2.41	66.55
DM	Porifera (P.) sp. 5	0.2	0.29	1.5	0.55	1.98	68.53
DM	Porifera (P.) sp. 22	0.2	0.25	1.43	0.51	1.89	70.43
LM	Actinaria (O.) spp.	1.91	1.84	6.08	1.16	8.59	8.59
LM	Actinaria (O.) sp. 4	1.25	1.2	4.93	1.11	6.97	15.57
LM	Unidentified 33	1.13	1.45	4.85	1.05	6.85	22.42
LM	Serpulidae (F.) spp.	0.97	1.17	4.53	1.06	6.41	28.83

LM	Unidentified 22	0.76	0.68	3.64	0.92	5.14	33.97
LM	Porifera (P.) sp. 4	0.68	0.83	3.45	0.98	4.88	38.85
LM	Unidentified 12	0.54	0.62	3.02	0.88	4.27	43.12
LM	Hymedesmiidae (F.) sp. 4	0.42	0.71	2.9	0.83	4.1	47.22
LM	Unidentified 25	0.64	0.42	2.88	0.8	4.07	51.28
LM	Pandalidae (F.) spp.	0.48	0.6	2.76	0.85	3.9	55.19
LM	Actinaria (O.) sp. 9	0.2	0.51	2.2	0.56	3.11	58.3
LM	Unidentified 28	0.34	0.44	2.02	0.74	2.86	61.16
LM	Zoantharia (O.) spp.	0.3	0.24	1.9	0.53	2.69	63.85
LM	Zoantharia (O.) sp. 2	0.29	0.17	1.73	0.43	2.44	66.29
LM	Unidentified 52	0.3	0.31	1.65	0.61	2.34	68.63
LM	Porifera (P.) sp. 22	0.21	0.25	1.39	0.52	1.97	70.6

The first- and second-order polynomial of coverage (%) were both significant ($p < 0.001$) for the final GLMMs with species richness and abundance as response variables (Table 8). Only the binomial GLM with Shannon diversity (*H*') as the response variable managed to successfully include both coverage of hard substrate (%) and the condition of *V. pourtalesii* as predictors (evident by the stability of the parameters in model selection, see Table D). Pielou evenness *J'* between areas with different states of *V. pourtalesii* was tested using a Kruskal-Wallis H test, adjusted for ties, after GLMMs (with quasi-poisson distributions and log link functions) failed to account for severe underdispersion ($\varphi \approx 0.016$), poor predictions, and, attempts to fit a binary logistic regression model led to quasi-complete separation (see Webb, Wilson & Chong, 2004). Differences in Pielou evenness *J'* between dead (median, IQR: 0.84, 0.73-0.92, $n_1 = 78$), live (median, IQR: 0.87, 0.79-0.93, $n_2 = 70$) and mixed (median, IQR: 0.88, 0.82-0.92, $n_3 = 135$) conditions of *V. pourtalesii* were not statistically significant ($\chi^2(2) = 4.83$, $p \approx 0.08$, $n = 273$, two-tailed; Fig. 10). The condition of *V. pourtalesii* was a statistically significant predictor of the species richness and abundance (GLMMs, $p < 0.002$, Fig. 10); however, the difference between live and dead assemblages was not statistically significant GLMM, $p > 0.15$).

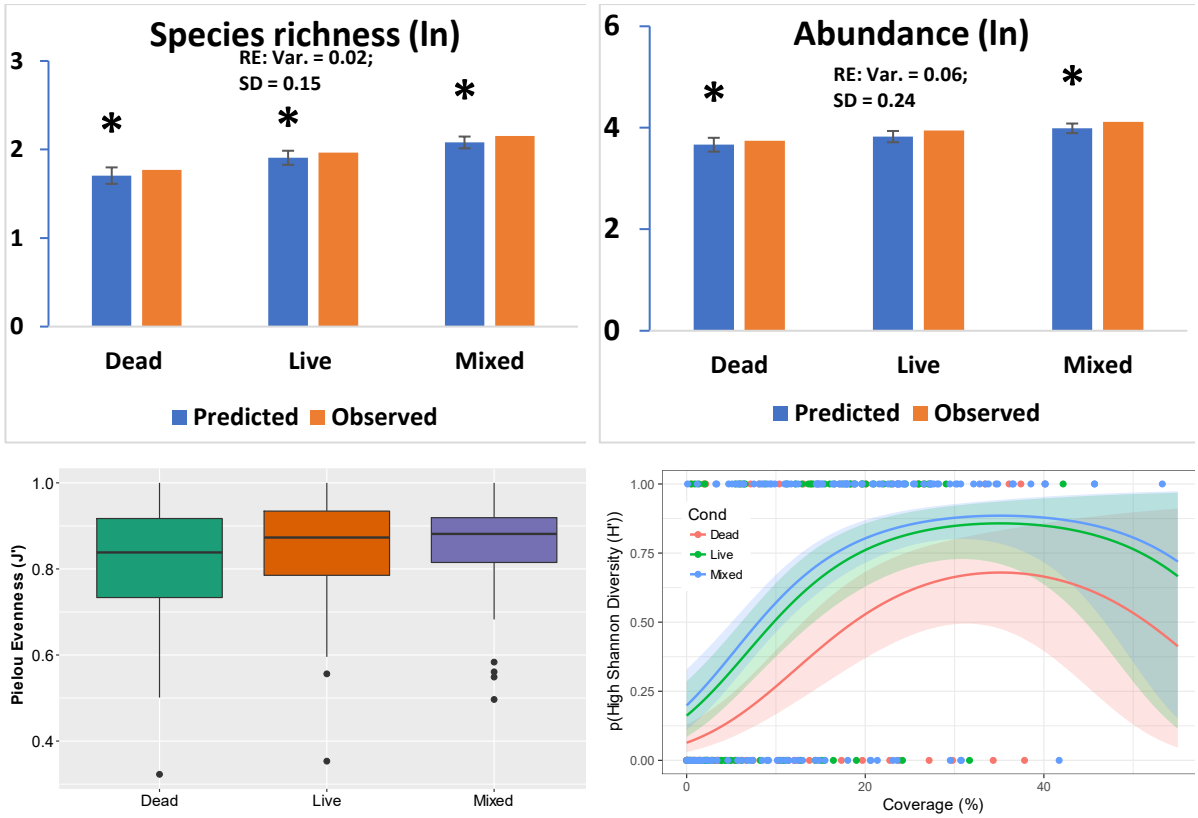

Fig. 10. Relationship between the condition of *V. pourtalesii* and the biodiversity indices. The observed and predicted values are compared to assess the validity of the predictions for the GLMMs of species richness and abundance. Shannon diversity (H') GLM is a probability model of high Shannon diversity (H'). Pielou evenness *J'* is compared amongst different assemblages of *V. pourtalesii*. Asterisks indicate significant differences. "RE" refers to the random effect and the variance and standard deviation of the random effect. "RE" refers to the random effect with "Var." and "SD denoting the variance and standard deviation of the random effect.

Table 8.
Summary of the final GLMMs with coverage (%) as a predictor of the respective biodiversity indices: species richness, abundance and Shannon (H') diversity (n = 290 for all models). "Coeff." is the shortened term for the coefficients of the GLMMs and "SE" the standard error. The random effects of each respective model are listed in the table, along with the variance and standard deviation of the respective random effects. The link in parentheses denotes the link function used.

Fixed effects	β	SE	*Z* score	*P*-value	Random effect	Var.	SD
Species richness (poisson distribution, link = log)							
Intercept	1.91	0.065	29.3	$< 2.0 \times 10^{(-16)}$	CON (5 transects)	0.016	0.127
Cov.	6.01	0.40	15.1	$< 2.0 \times 10^{(-16)}$			
Cov.^{2}	-1.93	0.36	-5.35	$< 8.91 \times 10^{(-8)}$			
Abundance (negative binomial distribution, link = log)							
Intercept	3.80	0.11	35.4	$< 2.0 \times 10^{(-16)}$	CON (5 transects)	0.049	0.22
Cov.	7.91	0.60	13.2	$< 2.0 \times 10^{(-16)}$			
Cov.^{2}	-2.27	0.53	-4.24	$< 2.19 \times 10^{(-5)}$			

Influence of substrate on *Vazella pourtalesii*

Only one live specimen of *Vazella pourtalesii* was observed on soft substrate in 442 counts, although the hard substrate may have been obscured by its lateral position (DSC-2011-06-09 193752.JPG). To determine if there were differences in the percentage coverage of hard substrate between areas with and without *V. pourtalesii*, a Mann-Whitney U test was conducted with continuity correction in R. The percentage coverage of hard substrate was significantly higher in areas with *V. pourtalesii* present (median, IQR:) compared to areas absent (median, IQR:) of *V. pourtalesii* (Mann-Whitney *U* = 162460, $p < 0.001$, n = 467, two-tailed; Fig 11). A Kruskal-Wallis test was also conducted to

determine if there were differences in coverage of hard substrate between the assemblages of *V. pourtalesii*. Following the rejection of the null hypothesis of the Kruskal-Wallis test (χ^2 (2) = 27.86, p < 0.001, n = 290), pair-wise differences were determined using Dunn's tests with Bonferroni-adjusted p-values. Statistically significant differences were found between live and mixed (z_i = -3.160, p < 0.001, n = 208), and dead and mixed (z_i = -5.08, p < 0.001, n = 217) assemblages of *V. pourtalesii*.

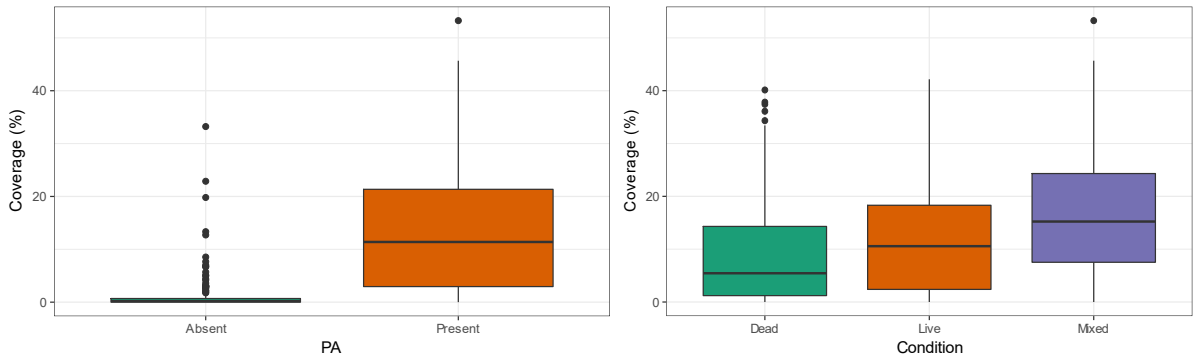

Fig. 11. Relationship between percentage coverage of hard substrate and the categorical predictors.

Discussion

Generally, as depth increases along continental margins, a corresponding decrease in abiotic (substrate variability, grain size and bottom current) and biotic (food supply and the size of epibenthic fauna) features are also found (Buhl-Mortensen *et al.*, 2010, and references therein). The provision of habitats with higher complexity, in areas that would otherwise be more homogenous, is one of the reasons why sponge grounds are increasingly recognised as key marine habitats (Maldonado *et al*., 2016; Hogg *et al*., 2010). The ecological functions of sponge grounds (Bell, 2008; Maldonado *et al.*, 2016), in particular the increased number of habitats of relatively high complexity due to the aggregations of sponges, are also of profound importance. The corresponding increases in surface area and the complexity and availability of niches, stemming from the aggregations of sponges can, in turn, result in enhanced diversity and abundance of resident fauna (Wulff, 2006; Buhl-Mortensen *et al*., 2010). Although a few studies have now looked at the relationship between sponge grounds and the associated epibenthic megafauna of the northwest Atlantic (Beazley *et al.*, 2013; Murillo *et al.*, 2012; Beazley *et al.*, 2015), only Korabik (2016) has specifically looked at small scale effects of *Vazella pourtalesii* and associated epibenthic megafauna in the Emerald Basin. Although this was the second quantitative assessment of *Vazella pourtalesii* and the associated epibenthic megafauna, it was the first quantitative assessment that also explored the effect of habitat complexity generated by geological processes, which also can also enhance the diversity of local fauna (Lacharité & Metaxas, 2017).

Vazella pourtalesii was found in all transects of this study, with the highest total abundance of the sponge occurring in CON 19, 20 and 5, respectively. These transects also had a higher mean and total abundance of taxa, as well as a higher number of rare taxa (Table 4). Both the predicted and observed biodiversity (species richness and Shannon diversity (H')) and abundance per photo were also higher when *V. pourtalesii* was present (Fig. 9). Thus, the results clearly show enhanced biodiversity in areas of sponge habitat compared to areas without sponges, which supports the previous work by (Korabik, 2016) and the first hypothesis. Pielou evenness *J'* was not a particularly useful biodiversity index when comparing areas with and without *V. pourtalesii*, as several photos in areas absent of *V. pourtalesii* had either few or no species present, resulting in failure to calculate the evenness. This was clearly reflected in the change in sample size, which dropped from 467 to 387 in total, but from 170 to 97 in areas absent of *V. pourtalesii*. Enhanced biodiversity and abundance has also been found in other sponge grounds of the northwest Atlantic: the multispecific sponge grounds in the Flemish Pass (Beazley *et al.*, 2013) and Sackville Spur (Beazley *et al*., 2015). Interestingly, although the species richness and total abundance were much higher in the multispecific sponge grounds of the Flemish Pass (Fig. 12), the relative differences in the magnitude of the same indices between areas with and without *V. pourtalesii* were much higher in this study. This is particularly evident when one compares the average abundance which was roughly 5 times higher in areas with *V. pourtalesii* present (Fig. 10). In the Flemish Pass (Beazley *et al.,* 2013) the abundance was only roughly twice as high in areas inside of the sponge grounds compared to areas outside of the sponge grounds (Fig. 12). It is important to note, however, that the definition of being inside a sponge ground was defined as having "structure-forming sponges present in a continuous or semi-continuous fashion" (Beazley *et al*., 2015), and therefore, the definitions are not equivalent (albeit procedurally similar). Nevertheless, the fact that such a strong local response was detected is very interesting. A possible explanation could be the very strong association between *V. pourtalesii* and hard substrate (Fig. 11) and the absence of other structure-forming of sponges on soft substrate (monospecific sponge grounds). Coverage of hard substrate was a statistically significant predictor of the diversity, abundance and presence of *V. pourtalesii*, whilst in the multispecific sponge grounds of the Flemish Cap (Beazley *et al*., 2013), several sponges also occurred on soft substrate (e.g. Demospongiae (C.) sp. 9; 36, 38; Porifera (P.) sp. 257). Habitat heterogeneity is a function of the complex interrelation between geologic, biogenic and disturbance factors (Kenchington, McLean and Rice, 2016); thus, areas absent of *V. pourtalesii* would also be likely to have low coverage of hard substrate, and in the absence of sponges or other organisms that can increase the local habitat complexity, the biodiversity and abundance would also likely be lower (i.e. the geologic and biogenic

effects are strongly correlated). In environments where the geologic effect is reduced, sponges can contribute by creating habitat heterogeneity that attracts and creates interactions with marine fauna (Wulff, 2006; Bell, 2008) and enhances the local biodiversity (Tissot *et al.*, 2006; Bo *et al.*, 2012). In the sponge grounds of the Sackville Spur, the larger Astrophorids often acted as substrate for other taxa such as ophiuroids and soft corals (Beazley *et al.*, 2015). An observation also reported by Klitgaard (1995) in her study of the fauna associated with sponges at the Faroe Islands. An important question is raised because of the strong correlation between the two effects: What is actually driving the differences in biodiversity and abundance? A future study examining areas without *V. pourtalesii* but with higher relative average substrate complexity than the values found in this study would help provide a more comprehensive answer. Considering the strong relationship between *V. pourtalesii* and substrate; however, perhaps an experimental approach would be better. Given the large number of zeroes in the absent group, particularly with species richness, future analyses could attempt to use zero-inflated GLMMs that take into account the potential autocorrelation of the data (e.g. Lee *et al*., 2006).

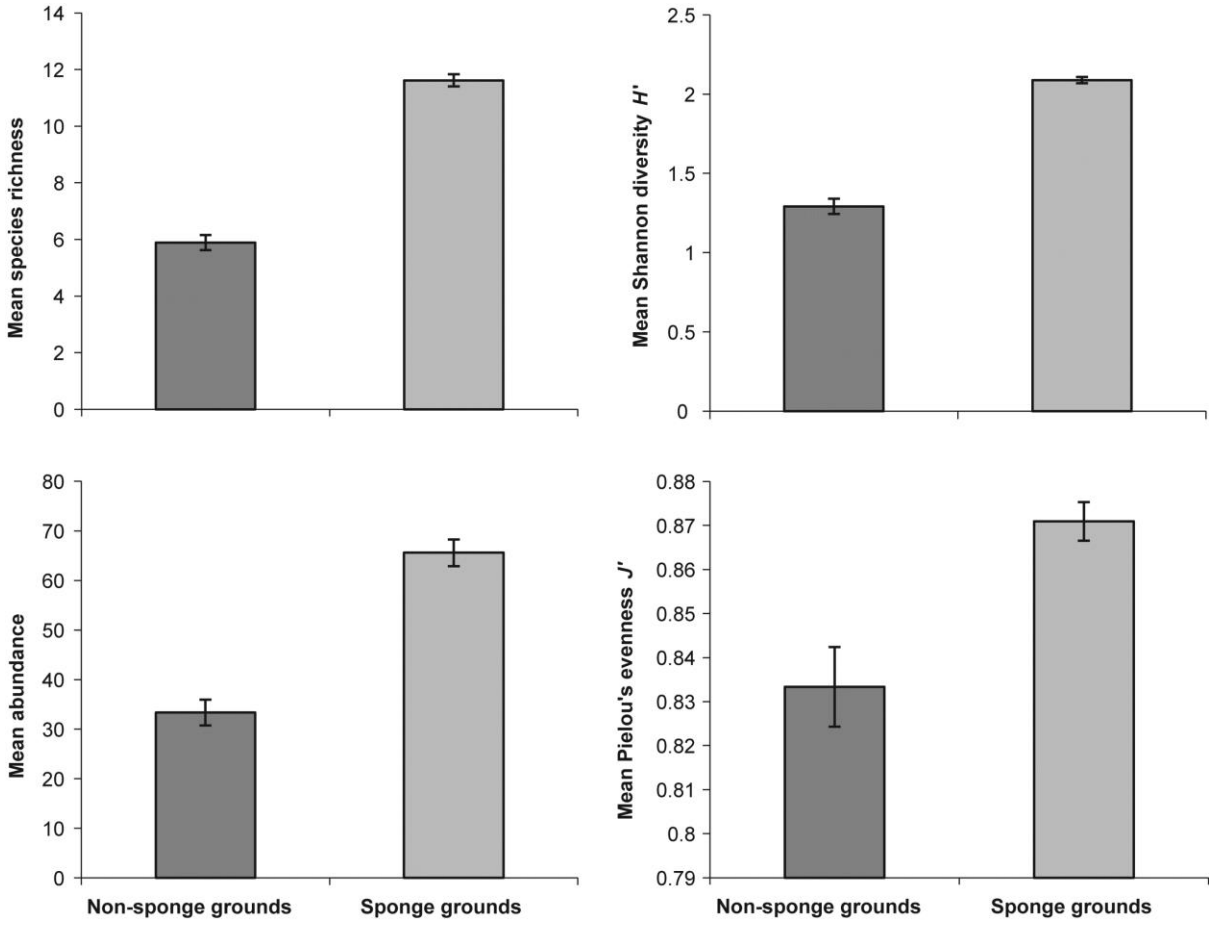

Fig. 12 (from Beazley *et al.*, 2014). Mean species richness, mean abundance, mean Shannon diversity *H'*, and mean Pielou's evenness *J'* per photo of epibenthic megafauna in the Flemish Pass. Error bars represent the standard error.

The composition of epibenthic megafauna differed significantly between areas with and without *V. pourtalesii*. Only one taxon, Zoantharia (O.) sp. 2, had a higher average abundance in areas absent of *V. pourtalesii*, and this colonial species was associated with soft substrate. Cross-examination of the MDS of the presence and absence of *V. pourtalesii* (Fig. 8) and transects (Fig. 9) revealed that the largest differences were primarily driven by images absent of *V. pourtalesii* in CON 18, 21 and 19, respectively. The largest differences in community composition were found between CON 18 and 20 (Table B3). The ANOSIM (Table B3) and SIMPER tests (Table B4) in conjunction with the summary table of transects (Table 4) offer one explanation: CON 18 had the lowest abundance, diversity, percentage coverage of hard substrate and total abundance of *V. pourtalesii*; with so few species in such a homogenous environment, community differences would likely be driven by whatever taxon or taxa that happened to be present. One could question the validity of the ANOSIM test in this instance, given its sensitivity to heterogeneity in dispersions (Walsh & Anderson, 2013). The SIMPER analysis still indicated that the community compositions were very different, as the three species that contributed to 70% of the similarity: Unidentified 33 (56.55%), Zoantharia (O.) sp. 2 (11.08%) and Pandalidae (F.) spp. (7.58%), were all taxa typically found on soft substrate. The previously discussed differences in biodiversity and abundance also support this. The SIMPER analysis (Table 6) also alludes to another interesting aspect to the sessile suspension feeders within the epibenthic communities associated with *V. pourtalesii*: What kind of interactions are found between these organisms? Competition for the limiting space of hard substrate is highly likely, yet these taxa were frequently observed in co-existence. Future ecological work should examine the nature of these interactions.

The condition of *V. pourtalesii* had effects on the biodiversity and abundance of epibenthic megafauna (Fig. 10); however, these differences were much smaller in magnitude than the differences between areas with and without *V. pourtalesii* (Fig. 9). The considerable overlap of the confidence intervals between live and dead assemblages in Shannon diversity (H'); however, would suggest that the differences would most likely not be statistically significant. Mixed assemblages of *V. pourtalesii* could enhance the biodiversity and abundance of epibenthic megafauna because they offer a larger variety of potential interactions between marine organisms (Wulff, 2006); however, another possibility, which by no means neglects the importance of the former argument, is that the response of diversity and abundance is related to the density of *V. pourtalesii*. The latter argument is convincing because of the definition used for mixed assemblages: combinations of live, dead or damaged *V. pourtalesii*. This alludes to something I did not consider until after the analyses were

conducted: mixed assemblages of *V. pourtalesii* would likely have higher densities of *V. pourtalesii* than the other assemblages. In their study of the multispecific sponge grounds (*Asconema foliata*, *Craniella* spp., Axinellidae and dominating Astrophorids) of the Sackville spur, Beazley and her colleagues (2015) found the largest turnover of megafaunal community composition at 15 structure-forming sponges per m^2. It would be very interesting to see if such a density effect could further explain the changes in biodiversity, abundance and community compositions found in this study. Coverage of hard substrate (%) was also a significant predictor of the biodiversity and abundance of this dataset (n = 290). This was also reflected in the results from the SIMPER analyses (Table 7, Table D2 and Table D3), as most of the taxa driving the differences between dead, live and mixed conditions of *V. pourtalesii* could be explained by substrate preference. This traces back to the question raised earlier: How we do know if *V. pourtalesii* is driving the differences? Although the GLM of Shannon diversity (H') included both parameters with condition as an additive effect, the different conditions of *V. pourtalesii* were associated with different levels of hard substrate. Future analyses that used the density of *V. pourtalesii* as a predictor based on a larger dataset (i.e. more confidence in the predictions) could perhaps answer the question.

Two closure areas with restrictions to bottom trawling were erected in 2013 as part of DFO's Policy for Managing the Impacts of Fishing on Sensitive Benthic Areas (DFO, 2014; 2015). Previous studies of *V. pourtalesii* have noted that it typically occurs on hard substrate (Fuller *et al.*, 2008; Fuller, 2011; Korabik, 2016); however, the results of this study support the idea that live specimens of *V. pourtalesii* must have hard substrate to survive. Past research indicates that sponges with upright massive morphologies are more susceptible to damage by trawling (Freese *et al*., 1999; Freese, 2001; Cook, Conway & Burd, 2008); and furthermore, that a full recovery, if even possible, is on a time frame of decades (Jones, 1992; Klitgaard & Tendal, 2004). Changes to the epibenthic community (Murillo *et al.*, 2012; De Leo *et al.*, 2017) and considerably lower epibenthic diversity and productivity (Kędra *et al.*, 2017) have also been observed. Whilst the direct effects of trawling on sponges have been studied extensively (e.g. Jones, 1992; Freese, 2001; 2003; Freese *et al.*, 1999; Cook, Conway & Burd, 2008), the indirect effects, such as the resuspension of sediment on deep-sea sponges (Tjensvoll *et al.*, 2013) remain relatively understudied. Considering the strong relationship between *V. pourtalesii* and hard substrate found in this study, two further implications may have to be considered from the effects of trawling: resuspension of sediment that subsequently covers hard substrate may have profound implications for recolonisation; and, the resuspension of sediment may also have direct effects on *V. pourtalesii* (e.g. a reduction in respiration, Tjensvoll *et al.*, 2013). The majority of images used in this study were obtained from transects primarily within the two

current areas with restrictions to bottom trawling in the Emerald Basin and Sambro Bank, which also have high densities of *V. pourtalesii* (Fuller, 2011). Recent modelling efforts by Kenchington *et al*., (2016) and Beazley *et al*., (2016); however, clearly indicate that areas with high densities and probabilities of *V. pourtalesii* extend far outside the range of the current protected areas (Fig. 13). Given the results of this study and the previous work by Korabik (2016) and Fuller (2011), more of this unique and vulnerable habitat should be protected.

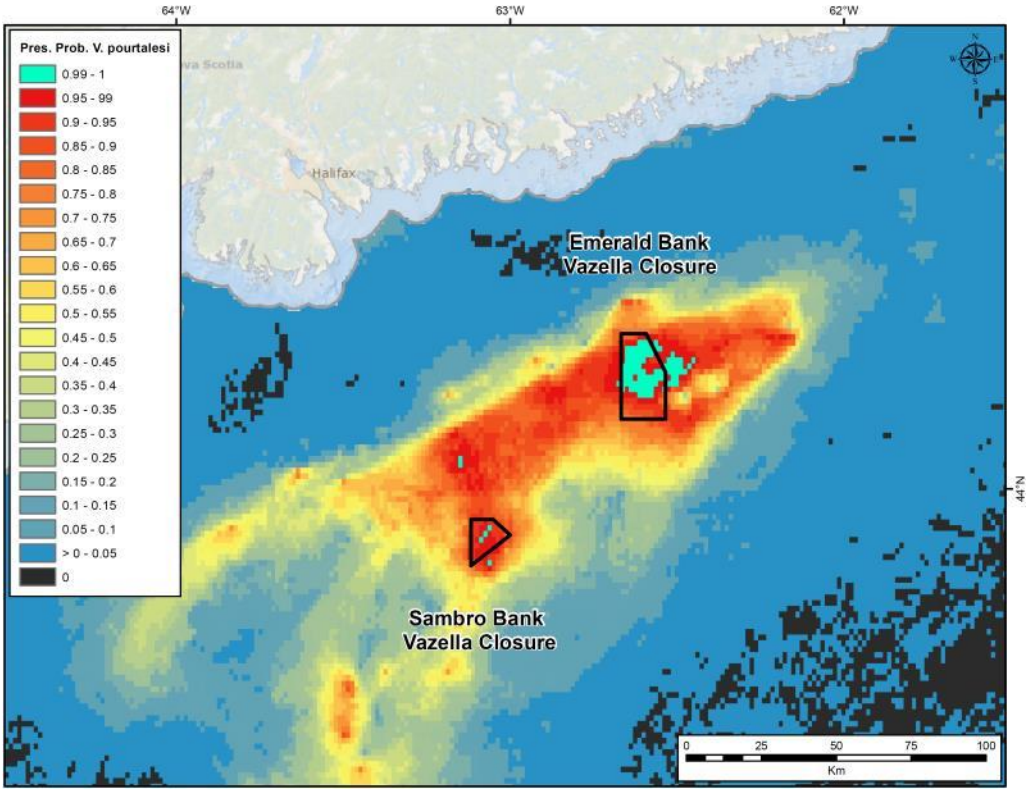

Fig. 13 (from Beazley *et al.*, 2016). Predictions of the presence probability of *V. pourtalesii* in Emerald Basin in relation to the two closure areas. Note that the areas of high probability fall outside the range of the current closure areas.

Conclusion

Although the models I used could be greatly improved and more data should still be collected, I believe the results of this study clearly show the important beneficial effects that *V. pourtalesii* has on the local epibenthic megafauna. The associations of *Sebastes* species and *Pollachius virens* with the *Vazella pourtalesii* sponge grounds (Fuller, 2011) also offer an impetus for protecting this vulnerable habitat. Furthermore, I only analysed one aspect of the observable biodiversity. Does fauna exist within the canals of the sponge (e.g. Padua, Lanna & Klautau, 2013; Erdman & Blake, 1987; Duarte & Nalesso, 1996)? How complex is the microbiota and what kind of interactions do they have (e.g. Thomas *et al.*, 2016)? What kind of effect do the spicule mats have on the local fauna (Bett & Rice, 1992; Barrio Froján *et al.*, 2012; Gutt, Böhmer & Dimmler, 2013)? It is easy to get lost in

the world of the unknown in regards to *Vazella pourtalesii*; however, it is important to act on what we do know already. Bottom trawling is arguably one of the most detrimental actions to the deep-sea floor considering its global distribution, frequency and intensity (Benn *et al.,* 2010; Ramirez-Llodra *et al.*, 2011). In the Emerald Basin, two key parties have to be taken into consideration: (i) the fisheries and (ii) the scientific community. A case can now be made that *Vazella pourtalesii* enhances the local diversity, abundance and composition of the epibenthic megafaunal communities; however, the primary interest of fisheries will always be the resource that they are dependent on. To this date (2017), only approximately 3% of the population is protected. A desirable solution (i.e. protecting more of this habitat) can only be achieved by capturing the interests of both parties. The association between *Sebastes* species and sponge grounds (Freese & Wing, 2003; Fuller, 2011) should be studied further, as it brings a powerful economic argument to the table.

Brendan Godley, an old professor of mine once remarked: “Conservation problems are people problems, and people problems require people solutions.”

References

Anderson, M. J. and Walsh, D. C., 2013. PERMANOVA, ANOSIM, and the Mantel test in the face of heterogeneous dispersions: what null hypothesis are you testing?. *Ecological Monographs*, 83 (4), pp: 557-574.

Barrio Froján, C. R. S., MacIsaac, K. G., McMillan, A. K., Sacau Cuadrado, M. M., Larege, P. A., *et al.* 2012. An evaluation of benthic community structure in and around the Sackville Spur closed area (Northwest Atlantic) in relation to the protection of vulnerable marine ecosystems. *ICES Journal of Marine Science*, 69: 213−222.

Beazley, L. I. & Kenchington, E. L. 2015. Epibenthic Megafauna of the Flemish Pass and Sackville Spur (Northwest Atlantic) Identified from *In Situ* Benthic Image Transects. *Canadian Technical Report of Fisheries and Aquatic Science*, 3127, 504 pp.

Beazley, L. I., Kenchington, E., Murillo, F. J., Lirette, C., Guijarro, J., *et al.* 2016. Species Distribution Modelling of Corals and Sponges in the Maritimes Region for Use in the Identification of Significant Benthic Areas. *Canadian Technical Report of Fisheries and Aquatic Science,* 3172, 198 pp.

Beazley, L. I., Kenchington, E.L., Murillo, F.J., & Sacau, M.M. 2013. Deep-sea sponge grounds enhance diversity and abundance of epibenthic megafauna in the Northwest Atlantic. *ICES Journal of Marine Science*, 70: 1471–1490.

Beazley, L. I., Kenchington, E., Yashayaev, I., & Murillo, F.J. 2015. Drivers of epibenthic megafaunal composition in the sponge grounds of the Sackville Spur, northwest Atlantic. *Deep-Sea Research I*, 98: 102-114.

Bell, J.J. 2008. The functional role of marine sponges. *Estuarine, Coastal, and Shelf Science*, 79: 341-353.

Benn, A.R., Weaver, P.P., Billet, D.S., Van Den Hove, S., Murdock, A.P., *et al*. 2010. Human activities on the deep seafloor in the North East Atlantic: an assessment of spatial extent. *PloS one,* 5(9).

Bett B. J., & Rice, A. L. 1992. The influence of hexactinellid sponge (*Pheronema carpenteri*) spicules on the patchy distribution of macrobenthos in the Porcupine Seabight (bathyal NE Atlantic), *Ophelia*, 36, pp: 217-226.

Bo, M., Bertolino, M. Bavestrello, G., Canese, S., Giusti, M., *et al*. 2012. Role of deep sponge grounds in the Mediterranean Sea: a case study in southern Italy. *Hydrobiologia*, 687, pp: 163-177.

Bolker, B. M., Brooks, M. E., Clark, C. J., Geange, S. W., Poulsen, J. R., *et al*. 2009. Generalized linear mixed models: a practical guide for ecology and evolution. *Trends in ecology & evolution*, 24 (3), pp: 127-135.

Buhl-Mortensen, L., Vanreusal, A., Gooday, A. J., Levin, L. A., Priede, I. G., *et al.* 2010. Biological structures as a source of habitat heterogeneity and biodiversity on the deep ocean margins. *Marine Ecology*, 31: 21-50.

Cárdenas, P., Pérez, T., & Boury-Esnault, N. (2012) "2 Sponge Systematics Facing New Challenges.", in Becerro, M. A., Uriz, M. J., Maldonado, M., & Turon, X. (eds) *Advances in marine biology*, 61, 79 - 209.

Clarke, K. R., Gorley, R. N. (2006) *PRIMER v6: User Manual/Tutorial*. PRIMER-E, Plymouth, 192pp.

Clarke, K. R., & Warwick R. M. (2001). *Change in marine communities: an approach to statistical analysis and interpretation*, 2nd edition. PRIMER-E, Plymouth, 172pp.

Conover, W. J. and Iman, R. L. (1979). On multiple-comparisons procedures. *Technical Report* LA-7677-MS, Los Alamos Scientific Laboratory.

Cook, S. E., Conway, K. W., and Burd, B. 2008. Status of the glass sponge reefs in the Georgia Basin. *Marine Environmental Research*, 66: S80-S86.

Costa, M. F. D. B., Mansur, K. F. R. and Leite, F. P. P., 2015. Temporal variation of the gammaridean fauna (Crustacea, Amphipoda) associated with the sponge *Mycale angulosa* (Porifera, Demospongiae) in southeastern Brazil. *Nauplius*, 23 (1), pp: 79-87.

De Leo, F. C., Gauthier, M., Nephin, J., Mihály, S., & Juniper, S. K., 2017. Bottom trawling and oxygen minimum zone influences on continental slope benthic community structure off Vancouver Island (NE Pacific). *Deep Sea Research Part II: Topical Studies in Oceanography*, 137, pp.404-419.

DFO. 2014. Offshore ecologically and biologically significant areas in the Scotian Shelf bioregion. DFO Canadian Science Advisory Secretariat Science Advisory Report 2014/041.

DFO. 2015. Coral and sponge strategy for Eastern Canada for 2015. (Accessed at: http://www.dfo-mpo.gc.ca/oceans/publications/cs-ce/index-eng.html)

Diaz, M. C., & Rützler, K., 2001. Sponges: an essential component of Caribbean coral reefs. *Bulletin of Marine Science*, 69 (2), pp: 535-546.

Dohrmann, M., Kelley, C., Kelly, M., Pisera, A., Hooper, J. N. and Reiswig, H. M., 2017. An integrative systematic framework helps to reconstruct skeletal evolution of glass sponges (Porifera, Hexactinellida). *Frontiers in zoology*, 14 (1), p.18.

Duarte, L. and Nalesso, R. 1996. The sponge *Zygomycale parishii* (Bowerbank) and its endobiotic fauna. *Estuarine, Coastal and Shelf Science*, 42, pp: 139-151.

Erdman, R. B. and Blake, N. J., 1987. POPULATION DYNAMICS OF THE SPONGE-DWELLING ALPHEID *SYNALPHEUS LONGICARPUS*, WITH OBSERVATIONS ON *S. BROOKSI* AND *S. PECTINIGER*, IN SHALLOW-WATER ASSEMBLAGES OF THE EASTERN GULF OF MEXICO. *Journal of Crustacean Biology*, 7 (2), pp: 328-337.

Fang, J. K., Schönberg, C. H., Hoegh-Guldberg, O., & Dove, S., 2017. Symbiotic plasticity of Symbiodinium in a common excavating sponge. *Marine Biology*, 164 (5), p.104.

Freese, J. L. 2001. Trawl-induced damage to sponges observed from a research submersible. *Marine Fisheries Review*, 63: 7–13.

Freese, J. L., & Wing, B. L. 2003. Juvenile red rockfish Sebastes sp., associations with sponges in the Gulf of Alaska. *Marine Fisheries Review*, 65: 38−42.

Freese, L., Auster, P. J., Heifetz, J., & Wing, B. L. 1999. Effects of trawling on seafloor habitat and associated invertebrate taxa in the Gulf of Alaska. *Marine Ecology Progress Series*, 182: 119–126.

Fuller, S. D., Murillo Perez, F. J., Wareham, V., and Kenchington, E. 2008. Vulnerable marine ecosystems dominated by deep-water corals and sponges in the NAFO convention area. NAFO SCR Doc. No. 08/22, Serial No. N5524. 24 pp.

Fuller, S. D. 2011. Diversity of marine sponges in the Northwest Atlantic, Ph.D. thesis, Dalhousie University, Halifax. 215 pp.

Goodwin, C. E., Berman, J., Downey, R. V., & Hendry, K. R., 2017. Carnivorous sponges (Porifera: Demospongiae: Poecilosclerida: Cladorhizidae) from the Drake Passage (Southern Ocean) with a description of eight new species and a review of the family Cladorhizidae in the Southern Ocean. *Invertebrate Systematics*, 31 (1), pp.37-64.

Gutt, J., Böhmer, A., & Dimmler, W. (2013). Antarctic sponge spicule mats shape macrobenthic diversity and act as a silicon trap. *Marine Ecology Progress Series*, 480, pp: 57–71.

Hestetun, J. T., Vacelet, J., Boury-Esnault, N., Borchiellini, C., Kelly, M. *et al.*, 2016. The systematics of carnivorous sponges. *Molecular phylogenetics and evolution*, 94, pp: 327-345.

Hogg, M. M., Tendal, O. S., Conway, K. W., Pomponi, S. A., van Soest, R. W. M., Gutt, J., Krautter, M*., et al.* 2010. Deep-sea Sponge Grounds: Reservoirs of Biodiversity. UNEP-WCMC Biodiversity Series, 32. UNEP-WCMC, Cambridge, UK. 86 pp.

Huang, J. P., McClintock, J. B., Amsler, C. D., & Huang, Y. M., 2008. Mesofauna associated with the marine sponge *Amphimedon viridis*. Do its physical or chemical attributes provide a prospective refuge from fish predation? J*ournal of Experimental Marine Biology and Ecology*, 362 (2), pp.95-100.

Jones, C. G., Lawton, J. H., and Shachak, M. 1994. Organisms as ecosystem engineers. *Oikos*, 69, pp: 373-386.

Kędra, M., Renaud, P. E., & Andrade, H., 2017. Epibenthic diversity and productivity on a heavily trawled Barents Sea bank (Tromsøflaket). *Oceanologia*, 59 (2), pp: 93-101.

Keigwin, L. D., Sachs, J. P. and Rosenthal, Y., 2003. A 1600-year history of the Labrador Current off Nova Scotia. *Climate Dynamics*, 21(1), pp.53-62.

Kenchington, E., Lirette, C., Cogswell, A., Archambault, D., Archambault, P., *et al.* 2010. Delineating coral and sponge concentrations in the biogeographic regions of the East Coast of Canada using spatial analyses. Canadian Science Advisory Secretariat (CSAS) Research Document, 2010/041. Fisheries and Oceans, Canada. 202 pp.

Kenchington, E., Lirette, C., Murillo, F. J., Beazley, L., Guijarro, J., *et al*. 2016. Kernel Density Analyses of Coral and Sponge Catches from Research Vessel Survey Data for Use in Identification of Significant Benthic Areas*. Canadian Technical Report of Fisheries and Aquatic Sciences*, 3167, 217 pp.

Kenchington, E., Link, H., Roy, V., Archambault, P. Siferd, T., *et al*. 2011. Identification of Mega- and Macrobenthic Ecologically Significant Areas (EBSAs) in the Hudson Bay Complex, the Western and Eastern Canadian Arctic. Canadian Science Advisory Secretariat (CSAS) Research Document, 2011/071. Fisheries and Oceans, Canada. 58 pp.

Kenchington, E., Mclean, S., & Rice, J. C. 2016. Considerations for Identification of Effective Area-based Conservation Measures. Canadian Science Advisory Secretariat (CSAS) Research Document, 2016/020. Fisheries and Oceans, Canada. 58 pp.

Kersken, D., Feldmeyer, B., & Janussen, D., 2016. Sponge communities of the Antarctic Peninsula: influence of environmental variables on species composition and richness. *Polar Biology*, 39 (5), pp.851-862.

King, L.H. and Fader, G.B., 1986. *Wisconsinan glaciation of the Atlantic continental shelf of southeast Canada* (No. 363). Geological Survey of Canada.

Klitgaard, A.B. 1995. The fauna associated with outer shelf and upper slope sponges (Porifera, Demospongiae) at the Faroe Islands, northeastern Atlantic. *Sarsia*, 80, pp: 1–22.

Klitgaard, A.B., & Tendal, O.S. 2004. Distribution and species composition of mass occurrences of large sponges in northeast Atlantic. *Progress in Oceanography*, 61, pp: 57-98.

Knudby, A., Kenchington, E., & Murillo, F.J., 2013. Modeling the distribution of *Geodia* sponges and sponge grounds in the Northwest Atlantic. *PloS one*, 8 (12).

Korabik, M. 2011. Epibenthic megafauna associated with Russian Hat (*Vazella pourtalesi*) sponge grounds, Emerald Basin, Scotian Shelf, BSc. thesis, Dalhousie University, Halifax. 45 pp.

Lacharité, M., & Metaxas, A., 2017. Hard substrate in the deep ocean: How sediment features influence epibenthic megafauna on the eastern Canadian margin. *Deep Sea Research Part I: Oceanographic Research Papers*.

Lee, A. H., Wang, K., Scott, J. A., Yau, K. K., & McLachlan, G. J., 2006. Multi-level zero-inflated Poisson regression modelling of correlated count data with excess zeros. *Statistical methods in medical research*, 15 (1), pp: 47-61.

Lind, K. F., Hansen, E., Østerud, B., Eilertsen, K. E., Bayer, A*, et al*. 2013. Antioxidant and anti-inflammatory activities of barettin. *Marine drugs*, 11 (7), pp: 2655-2666.

López-Acosta, M., Leynaert, A., & Maldonado, M., 2016. Silicon consumption in two shallow-water sponges with contrasting biological features. *Limnology and Oceanography*, 61 (6), pp: 2139-2150.

Lysek, N., Kinscherf, R., Claus, R., & Lindel, T. 2003. L-5-Hydroxytryptophan: Antioxidant and Anti-Apoptotic Principle of the Intertidal Sponge Hymeniacidon heliophila. *Zeitschrift für Naturforschung C*, 58 (7-8), pp: 568-572.

Maldonado, M., Aguilar, R., Bannister, R. J., Bell, J. J., Conway, K. W., *et al*. 2015. Sponge grounds as key marine habitats: a synthetic review of types, structure, functional roles, and conservation concerns. *Marine Animal Forests: The Ecology of Benthic Biodiversity Hotspots*, pp.1-39.

Manconi, R. and Pronzato, R., 2008. Global diversity of sponges (Porifera: Spongillina) in freshwater. *Hydrobiologia*, 595 (1), pp: 27-33.

Murillo, F.J., Durán Muñoz, P., Cristobo, J., Ríos, P., González, C., *et al.* 2012. Deep-sea sponge grounds of the Flemish Cap, Flemish Pass, and the Grand Banks of Newfoundland (Northwest Atlantic Ocean): distribution and species composition. *Marine Biology Research*, 8, pp: 842–854.

North Atlantic Fisheries Organisation 2009, *Report of the NAFO Scientific Council Working Group on Ecosystem Approach to Fisheries Management (WGEAFM).* NAFO SCS Doc. No. 09/6, Serial No. N5627. 25

O'hara, R. B., & Kotze, D. J., 2010. Do not log-transform count data. *Methods in Ecology and Evolution*, 1 (2), pp: 118-122.

Padua, A., Lanna, E. and Klautau, M., 2013. Macrofauna inhabiting the sponge Paraleucilla magna (Porifera: Calcarea) in Rio de Janeiro, Brazil. *Journal of the Marine Biological Association of the United Kingdom*, 93 (4), pp: 889-898.

Ramirez-Llodra, E., Tyler, P.A., Baker, M.C., Bergstad, O.A., Clark, M.R., *et al*. 2011. Man and the last great wilderness: human impact on the deep sea. *PLoS One*, 6 (8).

Reiswig, H. M., 2006. Classification and phylogeny of Hexactinellida (Porifera). *Canadian Journal of Zoology*, 84 (2), pp: 195-204.

Schmidt, O. 1870. Grundzüge einer Spongien-fauna des Atlantischen Gebietes. Engelmann, Leipzig, 88 pp.

Thomas, T., Moitinho-Silva, L., Lurgi, M., Björk, J. R., Easson, C., *et al*. 2016. Diversity, structure and convergent evolution of the global sponge microbiome. *Nature communications*, 7.

Tissot, B.N., Yoklavich, M.M., Love, M.S., York, K. and Amend, M., 2006. Benthic invertebrates that form habitat on deep banks off southern California, with special reference to deep sea coral. *Fishery Bulletin*, 104 (2), pp: 167-181.

Tjensvoll, I., Kutti, T., Fosså, J.H. and Bannister, R.J., 2013. Rapid respiratory responses of the deep-water sponge *Geodia barretti* exposed to suspended sediments. *Aquatic Biology*, 19 (1), pp: 65-73.

Wörheide, G., Dohrmann, M., Erpenbeck, D., Larroux, C., Maldonado, M., *et al*. (2012) "Deep Phylogeny and Evolution of Sponges (Phylum Porifera) in Becerro, M. A., Uriz, M. J., Maldonado, M., & Turon, X. (eds) *Advances in marine biology*, 61, 1 – 78.

Wulff, J. L. 2006. Ecological interactions of marine sponges. *Canadian Journal of Zoology*, 84, pp: 146–166.

Zuur, A. F., Ieno, E. N., Walker, N. J., Saveliev, A. A., & Smith, G. M. (2009) *Mixed Effects Models and Extensions in Ecology with R*. Springer Science+Business Media, New York. 574 pp.

Appendix

Appendix A

A1 – The Microsoft Access database

All tabs in the displayed form (Fig. 6) with downwards-pointing chevrons indicated a dropdown feature in each tab. “STATION:” gave you a dropdown menu with the imported CONs, i.e. CONs 18, 19, 20, 21 and 5. “PHOTO_FILE_NAME:” returned a list of all the imported images within that CON. Checking the “Process using Grid” box allowed one to activate or de-activate an additional tab in the form, “GRID LETTER:”, which also contained a dropdown feature with all of the grid cells (A-L). Once the correct CON, photo and grid letter were selected, the appropriate phylum (“SELECT PHYLUM:”), taxon (“SELECT TAXA:”) and the abundance (“COUNT:”) could be selected or input manually in their respective dropdown menus and added using the “Add Photo Data” tab. The “COMMENTS:” field allowed one to write comments about a specific entry in the database. After adding the photo data, the respective dropdown menus, i.e. “SELECT PHYLUM:”, “SELECT TAXA:”, “COUNT:” and “COMMENTS:”) were cleared, and this process was repeated for the remaining entries within the respective grid letter. The “ClearAll Data From Form” tab would clear all of the data currently input in all of the fields (Fig. 6), which proved to be a useful feature when reviewing the data, as one had to switch CON and photos frequently.

Appendix B

Table B1. Summary of pair-wise Dunn's tests (Bonferroni-adjusted p-values). Centred hyphen refers to the first respective labelled biodiversity index. Asterisk indicates statistical significance. All pair-wise tests were conducted in SPSS.

Biodiversity index	CONs	Test stastistic	Standard error	Adjusted significance
Species richness	CON 18 – CON 21	-55.194	23.108	0.169
-	CON18 – CON 19	-162.659	20.443	*
-	CON 18 – CON 20	-205.851	21.248	*
-	CON 18 – CON 5	-225.576	25.496	*
-	CON 21 – CON 19	107.465	18.661	*
-	CON 21 – CON 20	150.657	19.540	*
-	CON 21 – CON 5	-170.381	24.092	*
-	CON 19 – CON 20	-43.192	16.302	0.081
-	CON 19 – CON 5	-62.917	21.548	*
-	CON 20 – CON 5	-19.724	22.314	1.000
Abundance	CON 18 – CON 21	-26.543	23.165	1.000
-	CON18 – CON 19	-141.540	20.493	*
-	CON 18 – CON 20	-210.257	21.300	*
-	CON 18 – CON 5	-214.488	25.559	*
-	CON 21 – CON 19	114.997	18.707	*
-	CON 21 – CON 20	183.714	19.589	*
-	CON 21 – CON 5	-187.946	24.151	*
-	CON 19 – CON 20	-68.717	16.342	*
-	CON 19 – CON 5	-72.949	21.601	*
-	CON 20 – CON 5	-4.232	22.369	1.000
Pielou evenness *J'*	CON 20 – CON 18	10.325	27.281	1.000
-	CON 20 – CON 5	-39.519	18.805	0.356
-	CON 20 – CON 19	51.749	14.080	*
-	CON 20 – CON 21	-126.265	18.018	*
-	CON 18 – CON 5	-29.194	29.648	1.000
-	CON 18 – CON 19	-41.424	26.900	1.000
-	CON 18 – CON 21	-115.940	29.155	*
-	CON 5 – CON 19	12.230	18.247	1.000
-	CON 5 – CON 21	86.746	21.433	*
-	CON 19 – CON 21	-74.516	17.435	*
Shannon diversity (H')	CON 18 – CON 21	-67.690	23.121	*
-	CON18 – CON 19	-168.033	20.454	*
-	CON 18 – CON 20	-188.182	21.260	*
-	CON 18 – CON 5	-227.411	25.511	*
-	CON 21 – CON 19	100.343	18.672	*
-	CON 21 – CON 20	120.492	19.551	*
-	CON 21 – CON 5	-159.721	24.105	*
-	CON 19 – CON 20	-20.149	16.311	1.000
-	CON 19 – CON 5	-59.378	21.560	0.059
-	CON 20 – CON 5	-39.229	22.326	0.789

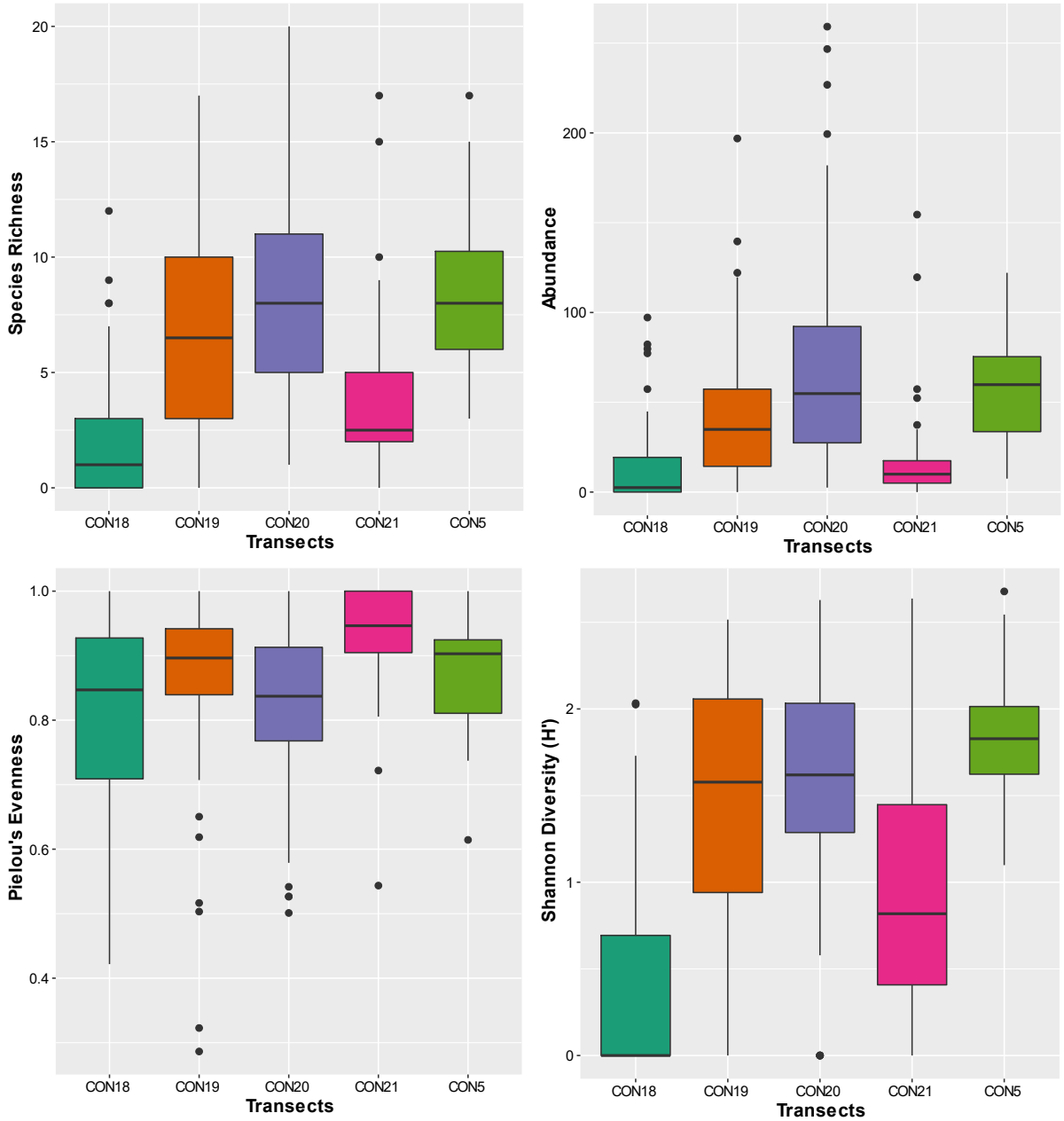

Fig. B2. Box plots (medians and IQRs) of the four biodiversity indices (species richness, abundance, Pielou evenness *J'* and Shannon diversity) by transect.

Table B3. Summary of pair-wise Dunn's tests (Bonferroni-adjusted p-values) testing for differences in hard substrate coverage (in %) between transects. Asterisk indicates statistical significance.

Pair-wise CONs	Test statistic	Standard error	Adjusted significance
CON 21 – CON 18	7.462	23.153	1.000
CON 21 – CON 19	118.019	18.698	*
CON 21 – CON 20	125.966	19.579	*
CON 21 – CON 5	-255.423	24.139	*
CON 18 – CON 19	-110.558	20.483	*
CON 18 – CON 20	-118.504	21.290	*
CON 18 – CON 5	-247.962	25.546	*
CON 19 – CON 20	-7.946	16.334	1.000
CON 19 – CON 5	-137.404	21.591	*
CON 20 – CON 5	-129.457	22.358	*

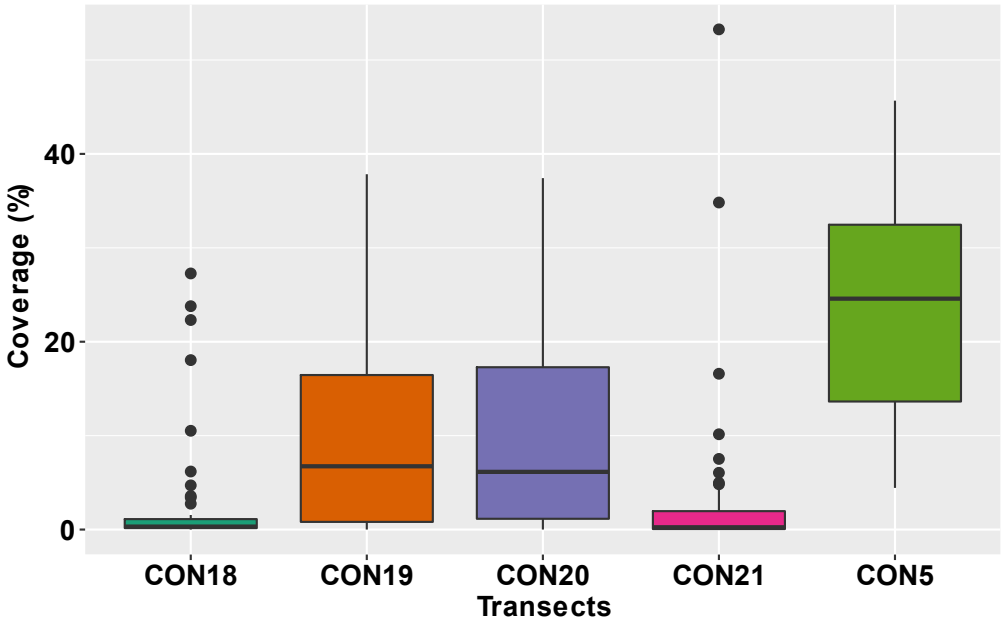

Fig. B4. Coverage of hard substrate (%) between transects.

Appendix C

Table C1. Taxa contributing up to 100% of the average dissimilarity between areas with and without *Vazella pourtalesii* present. Average abundances are based on the scale of the input data sheet (i.e. the log-transformed species-abundance matrix). Average dissimilarity is the contribution of the respective taxa to the total average dissimilarity (87.53%) between areas with and without *V. pourtalesii.* Multiplying the respective fractions by 100 gives the contribution values in percent listed below. The cumulative contribution in percent is simply a step-wise summarisation of the contribution (%) values.

Taxa	Average abundance – *V. pourtalesii* present	Average abundance – *V. pourtalesii* absent	Average dissimilarity	Standard deviation	Contribution (%)	Cumulative contribution (%)
Unidentified 33	1.43	0.7	9.47	0.84	10.82	10.82
Actinaria (O.) spp.	1.59	0.3	8.88	1.08	10.14	20.96
Serpulidae (F.) spp.	1.05	0.3	6.64	0.89	7.59	28.55
Actinaria (O.) sp. 4	1.02	0.18	5.63	0.85	6.43	34.98
Pandalidae (F.) spp.	0.55	0.26	4.15	0.69	4.74	39.72
Porifera (P.) sp. 4	0.7	0.07	3.8	0.67	4.34	44.06
Unidentified 12	0.58	0.15	3.77	0.67	4.3	48.37
Zoantharia (O.) sp. 2	0.28	0.33	3.74	0.51	4.27	52.64
Zoantharia (O.) spp.	0.28	0.22	3.14	0.43	3.59	56.23
Unidentified 25	0.48	0.12	2.96	0.58	3.39	59.61
Unidentified 22	0.51	0	2.93	0.53	3.34	62.96
Actinaria (O.) sp. 9	0.46	0.05	2.74	0.47	3.13	66.09
Hymedesmiidae (F.) sp. 4	0.5	0.03	2.34	0.56	2.68	68.77
Unidentified 28	0.34	0.06	1.74	0.53	1.99	70.76
Unidentified 61	0.15	0.16	1.65	0.44	1.88	72.64
Unidentified 21	0.19	0.07	1.47	0.37	1.68	74.32
Malacostraca (C.) spp.	0.09	0.14	1.45	0.37	1.65	75.97
Porifera (P.) sp. 22	0.22	0.04	1.23	0.38	1.41	77.38
Unidentified 52	0.25	0	1.13	0.39	1.3	78.67
Unidentified 80	0.12	0.08	1.06	0.32	1.21	79.88
Porifera (P.) sp. 8	0.19	0.02	0.99	0.36	1.13	81.01
Porifera (P.) sp. 5	0.21	0	0.99	0.36	1.13	82.14
Unidentified 103	0.18	0.03	0.95	0.38	1.08	83.23
Ophiuroidea (C.) spp.	0.07	0.06	0.94	0.25	1.08	84.3
Zoantharia (O.) sp. 1	0.13	0.01	0.89	0.22	1.02	85.32
Porifera (P.) sp. 43	0.17	0.01	0.84	0.33	0.96	86.28
Unidentified 27	0.13	0.03	0.81	0.33	0.93	87.21
Flabellum (G.) spp.	0.07	0.03	0.77	0.17	0.88	88.09
Porifera (P.) sp. 1	0.15	0.01	0.76	0.32	0.87	88.96
Bryozoa (P.) sp. 1	0.1	0.03	0.75	0.28	0.86	89.82
Hymedesmiidae (F.) sp. 1	0.16	0	0.73	0.2	0.83	90.65
Unidentified 38	0.13	0.02	0.69	0.31	0.79	91.44
Pachycerianthus borealis	0.06	0.03	0.64	0.22	0.73	92.17
Unidentified 19	0.09	0.01	0.53	0.22	0.61	92.78
Porifera (P.) sp. 12	0.09	0.01	0.52	0.24	0.6	93.38
Porifera (P.) sp. 14	0.1	0	0.5	0.23	0.57	93.95
Porifera (P.) sp. 56	0.14	0	0.46	0.26	0.52	94.47
***Polymastia* (G.) spp.**	0.03	0.03	0.44	0.17	0.51	94.98

Porifera (P.) sp. 49	0.04	0	0.35	0.14	0.4	95.38
Unidentified 87	0.03	0.02	0.34	0.19	0.38	95.77
Malacostraca (C.) sp. 1	0.04	0.01	0.33	0.15	0.38	96.14
Ophiuroidea (C.) sp. 1	0	0.04	0.31	0.16	0.35	96.49
Unidentified 1	0.02	0.02	0.25	0.15	0.28	96.77
Unidentified 120	0.02	0.01	0.24	0.16	0.28	97.05
Unidentified 71	0.02	0.01	0.24	0.14	0.27	97.32
Unidentified 23	0.01	0.03	0.23	0.12	0.26	97.58
Porifera (P.) sp. 53	0.05	0	0.22	0.18	0.25	97.84
Unidentified 276	0.02	0.01	0.22	0.13	0.25	98.09
Actinopterygii (C.) sp. 2	0	0.03	0.21	0.14	0.24	98.33
Didemnidae (F.) sp. 1	0.03	0.01	0.21	0.13	0.24	98.57
***Sebastes* (G.) spp.**	0.03	0	0.2	0.1	0.22	98.79
Porifera (P.) sp. 29	0.04	0.01	0.18	0.18	0.21	99
Unidentified 208	0.01	0.01	0.18	0.1	0.21	99.21
Unidentified 185	0.03	0.01	0.17	0.15	0.19	99.4
Unidentified 174	0.01	0.01	0.16	0.14	0.19	99.59
Unidentified 250	0	0.01	0.1	0.09	0.11	99.7
Unidentified 29	0	0.01	0.08	0.08	0.1	99.8
Porifera (P.) sp. 51	0.02	0	0.08	0.1	0.09	99.89
Unidentified 30	0.01	0	0.06	0.08	0.06	99.95
Unidentified 196	0.01	0	0.04	0.08	0.05	100

Table C2. Taxa (≥ 1% of the total abundance in any one transect) contributing up to 70% of the average dissimilarity between areas with and without *Vazella pourtalesii* present. Average abundances are based on the scale of the input data sheet (i.e. the log-transformed species-abundance matrix). Average dissimilarity is the contribution of the respective taxa to the total average dissimilarity (86.87%) between areas with and without *V. pourtalesii.* Multiplying the respective fractions by 100 gives the contribution values in percent listed below. The cumulative contribution in percent is simply a step-wise summarisation of the contribution (%) values. The epibenthic megafaunal composition was significantly different between areas with and without *Vazella pourtalesii* present (ANOSIM, global $R = 0.349$, $p < 0.001$, n = 467, 999 permutations).

Taxa	Average abundance – *V. pourtalesii* present	Average abundance – *V. pourtalesii* absent	Average dissimilarity	Standard deviation	Contribution (%)	Cumulative contribution (%)
Unidentified 33	1.43	0.7	10.12	0.85	11.65	11.65
Actinaria (O.) spp.	1.59	0.3	9.45	1.08	10.87	22.52
Serpulidae (F.) spp.	1.05	0.3	7.19	0.85	8.27	30.79
Actinaria (O.) sp. 4	1.02	0.18	6.01	0.84	6.92	37.71
Pandalidae (F.) spp.	0.55	0.26	4.41	0.69	5.08	42.79
Porifera (P.) sp. 4	0.7	0.07	4.1	0.63	4.71	47.5
Unidentified 12	0.58	0.15	4	0.66	4.6	52.11
Zoantharia (O.) sp. 2	0.28	0.33	3.98	0.51	4.59	56.69
Zoantharia (O.) spp.	0.28	0.22	3.34	0.43	3.85	60.54
Unidentified 25	0.48	0.12	3.13	0.58	3.6	64.14
Unidentified 22	0.51	0	3.1	0.53	3.57	67.71
Actinaria (O.) sp. 9	0.46	0.05	2.89	0.47	3.33	71.04

Table C3. Taxa contributing up to 70% of the average dissimilarity between areas with and without *Vazella pourtalesii* present, including *Meganyctiphanes norvegica*. Average abundances are based on the scale of the input data sheet (i.e. the log-transformed species-abundance matrix). Average dissimilarity is the contribution of the respective taxa to the total average dissimilarity (86.92%) between areas with and without *V. pourtalesii.* Multiplying the respective fractions by 100 gives the contribution values in percent listed below. The cumulative contribution in percent is simply a step-wise summarisation of the contribution (%) values. The epibenthic megafaunal composition was significantly different between areas with and without *Vazella pourtalesii* present (ANOSIM, global R = 0.37, $p < 0.001$, n = 467, 999 permutations).

Taxa	Average abundance – *V. pourtalesii* present	Average abundance – *V. pourtalesii* absent	Average dissimilarity	Standard deviation	Contribution (%)	Cumulative contribution (%)
Meganyctiphanes norvegica	0.33	1.6	10.48	0.71	12.06	12.06
Unidentified 33	1.43	0.7	8.57	0.89	9.86	21.93
Actinaria (O.) spp.	1.59	0.3	8.44	1.09	9.71	31.64
Serpulidae (F.) spp.	1.05	0.3	6.07	0.93	6.98	38.62
Actinaria (O.) sp. 4	1.02	0.18	5.36	0.86	6.16	44.79
Pandalidae (F.) spp.	0.55	0.26	3.86	0.71	4.44	49.22
Porifera (P.) sp. 4	0.7	0.07	3.61	0.67	4.16	53.38
Zoantharia (O.) sp. 2	0.28	0.33	3.57	0.52	4.11	57.49
Unidentified 12	0.58	0.15	3.5	0.69	4.02	61.51
Zoantharia (O.) spp.	0.28	0.22	2.95	0.45	3.39	64.9
Unidentified 25	0.48	0.12	2.81	0.58	3.23	68.13
Unidentified 22	0.51	0	2.71	0.54	3.11	71.25

Appendix D

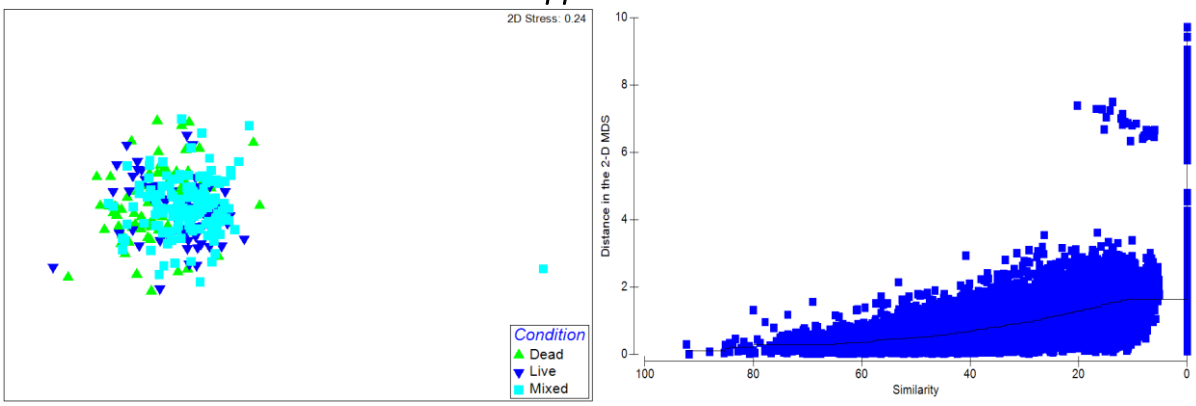

Fig. D1. MDS (left) of samples (n = 290) with dead, live and mixed specimens of *Vazella pourtalesii* depicted by green, blue and cyan shapes, respectively (stress = 0.24). The Shepard diagram (right) shows high levels of variance around the best-fit regression line, i.e. indicating that the rank order relationships are not exactly preserved (Clarke & Gorley, 2006).

Table D2. Following rejection of the null hypothesis of the one-way ANOSIM (ANOSIM, global $R = 0.105$, $p < 0.001$, n = 290, 999 permutations), pair-wise differences were further tested with new ANOSIMs, and the SIMPER routine was used to identify the taxa driving the differences. "Groups compared" refers to the respective pair-wise comparisons: DL refers to the comparison between samples with dead and live *V. pourtalesii*; DM refers to the comparison between samples with dead and mixed *V. pourtalesii*; and, LM refers to the comparison between samples with live and mixed *V. pourtalesii*. The average abundances of "Condition 1" and "Condition 2" refers to the respective order the groups listed in "Groups compared". Average abundances are based on the scale of the input data sheet (i.e. the log-transformed species-abundance matrix). Average dissimilarity is the contribution of the respective taxa to the respective total average dissimilarities (DL = 75.56%, DM = 74.28% and ML = 69.15%). Multiplying the respective fractions by 100 gives the contribution values in percent listed below. The cumulative contribution in percent is simply a step-wise summarisation of the contribution (%) values for the respective groups compared. DM field is only highlighted as a visual aid to separate the pair-wise comparisons.

Groups compared	Taxa	Average abundance – Condition 1	Average abundance – Condition 2	Average dissimilarity	Standard deviation	Contribution (%)	Cumulative contribution (%)
DL	Actinaria (O.) spp.	0.93	1.91	8.02	1.2	10.61	10.61
DL	Unidentified 33	1.66	1.13	6.55	1.03	8.67	19.28
DL	Serpulidae (F.) spp.	0.9	0.97	5.8	0.98	7.68	26.96
DL	Actinaria (O.) sp. 4	0.51	1.25	5.76	1	7.62	34.58
DL	Unidentified 12	0.55	0.54	3.82	0.84	5.06	39.64
DL	Porifera (P.) sp. 4	0.53	0.68	3.79	0.84	5.02	44.65
DL	Unidentified 25	0.45	0.64	3.74	0.8	4.95	49.61
DL	Unidentified 22	0	0.76	3.67	0.74	4.86	54.46
DL	Pandalidae (F.) spp.	0.52	0.48	3.21	0.82	4.25	58.71
DL	Zoantharia (O.) sp. 2	0.41	0.29	3.16	0.57	4.19	62.9
DL	Actinaria (O.) sp. 9	0.63	0.2	3.13	0.64	4.15	67.04
DL	Zoantharia (O.) spp.	0.32	0.3	2.69	0.54	3.56	70.6
DM	Actinaria (O.) spp.	0.93	1.84	7.18	1.21	9.67	9.67
DM	Unidentified 33	1.66	1.45	6.08	0.98	8.19	17.86
DM	Serpulidae (F.) spp.	0.9	1.17	5.45	1.05	7.34	25.2
DM	Actinaria (O.) sp. 4	0.51	1.2	5.07	1.04	6.82	32.02
DM	Porifera (P.) sp. 4	0.53	0.83	3.89	0.89	5.24	37.26

DM	Actinaria (O.) sp. 9	0.63	0.51	3.74	0.72	5.04	42.3
DM	Unidentified 12	0.55	0.62	3.53	0.85	4.75	47.04
DM	Pandalidae (F.) spp.	0.52	0.6	3.29	0.83	4.42	51.47
DM	Hymedesmiidae (F.) sp. 4	0.25	0.71	2.96	0.77	3.98	55.45
DM	Unidentified 25	0.45	0.42	2.83	0.71	3.81	59.26
DM	Unidentified 22	0	0.68	2.82	0.65	3.8	63.06
DM	Zoantharia (O.) sp. 2	0.41	0.17	2.51	0.57	3.38	66.45
DM	Zoantharia (O.) spp.	0.32	0.24	2.33	0.5	3.14	69.59
DM	Unidentified 28	0.18	0.44	1.94	0.64	2.61	72.2
LM	Actinaria (O.) spp.	1.91	1.84	6.47	1.16	9.36	9.36
LM	Actinaria (O.) sp. 4	1.25	1.2	5.25	1.11	7.59	16.95
LM	Unidentified 33	1.13	1.45	5.17	1.06	7.48	24.43
LM	Serpulidae (F.) spp.	0.97	1.17	4.84	1.06	7	31.43
LM	Unidentified 22	0.76	0.68	3.86	0.91	5.59	37.01
LM	Porifera (P.) sp. 4	0.68	0.83	3.67	0.98	5.31	42.32
LM	Unidentified 12	0.54	0.62	3.2	0.87	4.62	46.95
LM	Hymedesmiidae (F.) sp. 4	0.42	0.71	3.09	0.83	4.46	51.41
LM	Unidentified 25	0.64	0.42	3.06	0.8	4.42	55.83
LM	Pandalidae (F.) spp.	0.48	0.6	2.93	0.84	4.23	60.07
LM	Actinaria (O.) sp. 9	0.2	0.51	2.34	0.56	3.39	63.45
LM	Unidentified 28	0.34	0.44	2.14	0.74	3.1	66.55
LM	Zoantharia (O.) spp.	0.3	0.24	2.02	0.52	2.93	69.48
LM	Zoantharia (O.) sp. 2	0.29	0.17	1.84	0.43	2.66	72.13

Table D3. Following rejection of the null hypothesis of the one-way ANOSIM (ANOSIM, global $R = 0.107$, $p < 0.001$, n = 290, 999 permutations), pair-wise differences were further tested with new ANOSIMs, and the SIMPER routine was used to identify the taxa driving the differences. "Groups compared" refers to the respective pair-wise comparisons: DL refers to the comparison between samples with dead and live *V. pourtalesii*; DM refers to the comparison between samples with dead and mixed *V. pourtalesii*; and, LM refers to the comparison between samples with live and mixed *V. pourtalesii*. The average abundances of "Condition 1" and "Condition 2" refers to the respective order the groups listed in "Groups compared". Average abundances are based on the scale of the input data sheet (i.e. the log-transformed species-abundance matrix). Average dissimilarity is the contribution of the respective taxa to the respective total average dissimilarities (DL = 76.30%, DM = 74.96% and ML = 70.31%). Multiplying the respective fractions by 100 gives the contribution values in percent listed below. The cumulative contribution in percent is simply a step-wise summarisation of the contribution (%) values for the respective groups compared. DM field is only highlighted as a visual aid to separate the pair-wise comparisons.

Groups compared	Taxa	Average abundance – Condition 1	Average abundance – Condition 2	Average dissimilarity	Standard deviation	Contribution (%)	Cumulative contribution (%)
DL	Actinaria (O.) spp.	0.93	1.91	7.71	1.19	10.1	10.1
DL	Unidentified 33	1.66	1.13	6.14	1.04	8.04	18.14
DL	Actinaria (O.) sp. 4	0.51	1.25	5.51	1.03	7.22	25.37
DL	Serpulidae (F.) spp.	0.9	0.97	5.34	1.03	7	32.37
DL	*Meganyctiphanes norvegica*	0.24	0.64	4.26	0.44	5.58	37.94
DL	Unidentified 25	0.45	0.64	3.59	0.8	4.7	42.65
DL	Unidentified 12	0.55	0.54	3.57	0.85	4.68	47.33
DL	Porifera (P.) sp. 4	0.53	0.68	3.57	0.87	4.68	52.01
DL	Unidentified 22	0	0.76	3.43	0.75	4.49	56.49
DL	Actinaria (O.) sp. 9	0.63	0.2	3.02	0.64	3.96	60.45
DL	Pandalidae (F.) spp.	0.52	0.48	3.01	0.84	3.95	64.4
DL	Zoantharia (O.) sp. 2	0.41	0.29	3	0.57	3.93	68.34
DL	Zoantharia (O.) spp.	0.32	0.3	2.54	0.55	3.33	71.67
DM	Actinaria (O.) spp.	0.93	1.84	6.88	1.21	9.18	9.18
DM	Unidentified 33	1.66	1.45	5.81	0.98	7.75	16.94
DM	Serpulidae (F.) spp.	0.9	1.17	5.17	1.07	6.9	23.84
DM	Actinaria (O.) sp. 4	0.51	1.2	4.85	1.04	6.47	30.31
DM	Porifera (P.) sp. 4	0.53	0.83	3.74	0.9	4.99	35.29
DM	Actinaria (O.) sp. 9	0.63	0.51	3.63	0.71	4.85	40.14
DM	Unidentified 12	0.55	0.62	3.41	0.85	4.55	44.69
DM	Pandalidae (F.) spp.	0.52	0.6	3.15	0.83	4.2	48.89
DM	Hymedesmiidae (F.) sp. 4	0.25	0.71	2.85	0.78	3.81	52.7
DM	Unidentified 22	0	0.68	2.73	0.65	3.64	56.34
DM	Unidentified 25	0.45	0.42	2.72	0.71	3.62	59.97
DM	Zoantharia (O.) sp. 2	0.41	0.17	2.41	0.57	3.22	63.19
DM	Zoantharia (O.) spp.	0.32	0.24	2.23	0.5	2.98	66.16
DM	*Meganyctiphanes norvegica*	0.24	0.2	2.06	0.3	2.74	68.91
DM	Unidentified 28	0.18	0.44	1.88	0.63	2.51	71.42

LM	Actinaria (O.) spp.	1.91	1.84	6.09	1.16	8.67	8.67
LM	Actinaria (O.) sp. 4	1.25	1.2	4.96	1.12	7.06	15.72
LM	Unidentified 33	1.13	1.45	4.84	1.07	6.88	22.6
LM	Serpulidae (F.) spp.	0.97	1.17	4.52	1.09	6.43	29.03
LM	Unidentified 22	0.76	0.68	3.63	0.93	5.16	34.19
LM	Porifera (P.) sp. 4	0.68	0.83	3.49	0.98	4.96	39.16
LM	*Meganyctiphanes norvegica*	0.64	0.2	3.33	0.42	4.74	43.89
LM	Unidentified 12	0.54	0.62	3.03	0.88	4.3	48.2
LM	Hymedesmiidae (F.) sp. 4	0.42	0.71	2.95	0.83	4.2	52.4
LM	Unidentified 25	0.64	0.42	2.9	0.8	4.13	56.53
LM	Pandalidae (F.) spp.	0.48	0.6	2.78	0.85	3.95	60.47
LM	Actinaria (O.) sp. 9	0.2	0.51	2.22	0.56	3.16	63.63
LM	Unidentified 28	0.34	0.44	2.06	0.74	2.93	66.56
LM	Zoantharia (O.) spp.	0.3	0.24	1.9	0.52	2.71	69.27
LM	Zoantharia (O.) sp. 2	0.29	0.17	1.76	0.44	2.5	71.77

Appendix E

Table E1. Model selection with presence of *V.* pourtalesii as a predictor was conducted by selecting the models with the lowest AIC and checking the diagnostics of the respective models. Pearson chi-square tests were used to compare models separately (i.e. step-wise within the series of fixed or mixed effects models) and between the final fixed effects and mixed effects models (comp. refers to the models compared). Asterisk indicates statistical significance ($p < 0.05$). "Dist." denotes the distribution. The "best" models are in bold.

Dist.	Model	AIC	ΔAIC	χ^2 - within	χ^2 - across
Neg. bin.	**SR ~ Presence + (1|CON)**	**2247.8**	**comp.**	**153.8 ***	**69.1 ***
Neg. bin.	SR ~ +1 + (1|CON)	2399.6	151.8	-	-
Neg. bin.	SR ~ Presence	2314.9	67.1	236.6	comp.
Neg. bin.	SR~ +1	2549.5	301.7	-	-
Neg. bin.	**Abundance ~ Presence + (1|CON)**	**4052.9**	**comp.**	**184.7 ***	**82.8 ***
Neg. bin.	Abundance ~ +1 + (1|CON)	4235.9	183	-	-
Neg. bin.	Abundance ~ Presence	4133.7	80.8	210.8 *	comp.
Neg. bin.	Abundance ~ +1	4342.5	289.6	-	-
Bin.	**H2 ~ Presence + (1|CON)**	**530.0**	**comp.**	**49.1 ***	**17.1 ***
Bin.	H2 ~ +1 + (1|CON)	577.1	47.1	-	-
Bin.	H2 ~ Presence	545.1	15.1	106.3	comp.
Bin.	H2 ~ +1	649.4	119.4	-	-

Table E2. Model selection with percentage coverage of hard substrate as a predictor was conducted by selecting the models with the lowest AIC and checking the diagnostics of the respective models. Pearson chi-square tests were used to compare models separately (i.e. step-wise within the series of fixed or mixed effects models) and between the final fixed effects and mixed effects models (comp. refers to the models compared). Asterisk indicates statistical significance ($p < 0.05$). "Dist." denotes the distribution. The "best" models are in bold.

Dist.	Model	AIC	ΔAIC	χ^2 - within	χ^2 - across
Neg. bin.	**SR ~ poly(Cov, 2) + (1|CON)**	**2063.6**	**comp.**	**comp.**	**96.3 ***
Neg. bin.	SR ~ Cov + (1|CON)	2144.0	80.4	82.4 *	-
Neg. bin.	SR ~ +1 + (1|CON)	2399.6	336	339.9 *	-
Neg. bin.	SR ~ poly(Cov, 2)	2158.0	94.4	comp.	comp.
Neg. bin.	SR ~ Cov	2273.0	209.4	117 *	-
Neg. bin.	SR ~ +1	2549.5	485.9	395.5 *	-
Neg. bin.	**Abundance ~ poly(Cov, 2) + (1|CON)**	**4004.5**	**comp.**	**comp.**	**68.3 ***
Neg. bin.	Abundance ~ Cov + (1|CON)	4049.7	45.2	47.2 *	-
Neg. bin.	Abundance ~ +1 + (1|CON)	4235.6	231.1	235.1 *	-
Neg. bin.	Abundance ~ poly(Cov, 2)	4070.8	66.3	comp.	comp.
Neg. bin.	Abundance ~ Cov	4135.8	131.3	67.0 *	-
Neg. bin.	Abundance ~ +1	4342.5	338.0	275.7 *	-
Bin.	**H2 ~ poly(Cov, 2) + (1|CON)**	**408.0**	**comp.**	**comp.**	**5.01 ***
Bin.	H2 ~ Cov + (1|CON)	414.4	6.4	8.4 *	-
Bin.	H2 ~ +1 + (1|CON)	577.1	169.1	173.1	-
Bin.	H2 ~ poly(Cov, 2) + (1|CON)	411.0	3	comp.	comp.
Bin.	H2 ~ Cov + (1|CON)	419.8	11.8	10.8	-
Bin.	H2 ~ +1 + (1|CON)	649.4	241.8	242.4 *	-

Table E3. Model selection with the condition of *V.* pourtalesii as a predictor was conducted by selecting the models with the lowest AIC and checking the diagnostics of the respective models. Pearson chi-square tests were used to compare models separately (i.e. step-wise within the series of fixed or mixed effects models) and between the final fixed effects and mixed effects models (comp. refers to the models compared). Asterisk indicates statistical significance ($p < 0.05$). "Dist." denotes the distribution. The "best" models are in bold.

Dist.	Model	AIC	ΔAIC	χ^2 - within	χ^2 - across
Neg. bin.	**SR ~ Condition + (1|CON)**	**1528.9**	**comp.**	**31.5 ***	**7.12 ***
Neg. bin.	SR ~ +1 + (1|CON)	1556.1	27.2	-	-
Neg. bin.	SR ~ Condition	1534.0	5.1	31.3 *	comp.
Neg. bin.	SR~ +1	1561.4	32.5	-	-
Neg. bin.	**Abundance ~ Condition + (1|CON)**	**2803.7**	**comp.**	**11.6 ***	**19.0 ***
Neg. bin.	Abundance ~ +1 + (1|CON)	2811.3	7.6	-	-
Neg. bin.	Abundance ~ Condition	2820.7	17	14.0 *	comp.
Neg. bin.	Abundance ~ +1	2830.7	27	-	-

Table E4. Model selection with percentage coverage of hard substrate as a predictor was conducted by selecting the models with the lowest AIC and checking the diagnostics of the respective models. Pearson chi-square tests were used to compare models separately (i.e. step-wise within the series of fixed or mixed effects models) and between the final fixed effects and mixed effects models (comp. refers to the models compared). Asterisk indicates statistical significance ($p < 0.05$). "Dist." denotes the distribution. The "best" models are in bold.

Dist.	Model	AIC	ΔAIC	χ^2 - within	χ^2 - across
Poisson	**SR ~ poly(Cov, 2) + (1|CON)**	**1360.1**	**comp.**	**comp.**	**24.1 ***
Poisson	SR ~ Cov + (1|CON)	1388.6	28.5	30.5 *	-
Poisson	SR ~ +1 + (1|CON)	1602.1	242	246.1 *	-
Poisson	SR ~ poly(Cov, 2)	1382.1	22	comp.	comp.
Poisson	SR ~ Cov	1421.3	61.2	41.2 *	-
Poisson	SR ~ +1	1620.3	260.2	242.1 *	-
Neg. bin.	**Abundance ~ poly(Cov, 2) + (1|CON)**	**2670.8**	**comp.**	**comp.**	**35.1 ***
Neg. bin.	Abundance ~ Cov + (1|CON)	2685.0	14.2	16.3 *	-
Neg. bin.	Abundance ~ +1 + (1|CON)	2811.3	140.5	144.6 *	-
Neg. bin.	Abundance ~ poly(Cov, 2)	2703.8	33	comp.	comp.
Neg. bin.	Abundance ~ Cov	2723.1	52.3	21.3 *	-
Neg. bin.	Abundance ~ +1	2830.7	159.9	109.6 *	-

Table E5. Model selection with percentage coverage of hard substrate and condition as a predictor was conducted by selecting the models with the lowest AIC and checking the diagnostics of the respective models. Pearson chi-square tests were used to compare models separately (i.e. step-wise within the series of fixed or mixed effects models) and between the final fixed effects and mixed effects models (comp. refers to the models compared). Asterisk indicates statistical significance ($p < 0.05$). "Dist." denotes the distribution. The "best" model is in bold.

Dist.	Model	AIC	ΔAIC	χ^2 - within	χ^2 - across
Bin.	H2 ~ poly(Cov,2)*Condition + (1|CON)	321.0	comp.	-	-
Bin.	H2 ~ poly(Cov,2)+Condition + (1|CON)	313.3	-7.7	comp.	NA
Bin.	H2 ~ Cov *Condition + (1|CON)	320.8	-0.2	-	-
Bin.	H2 ~ Cov+Condition + (1|CON)	317.8	-3.2	6.5*	-
Bin.	H2 ~ Cov + (1|CON)	27.6	.6	-	-
Bin.	H2 ~ Condition + (1|CON)	376.9	55.9	-	-
Bin.	H2 ~+1 + (1|CON)	406.0	85	100.7 *	-
Bin.	H2 ~ poly(Cov,2)*Condition	319.0	-2	-	-
Bin.	**H2 ~ poly(Cov,2)+Condition**	**311.3**	**-9.7**	**comp.**	**comp.**
Bin.	H2 ~ Cov*Condition	318.8	-2.2	-	-
Bin.	H2 ~ Cov+Condition	315.8	-5.2	6.5 *	-
Bin.	H2 ~ Cov	328.5	7.5	-	-
Bin.	H2 ~ Condition	375.2	54.2	-	-
Bin.	H2~+1	404.0	83.0	100.7 *	-

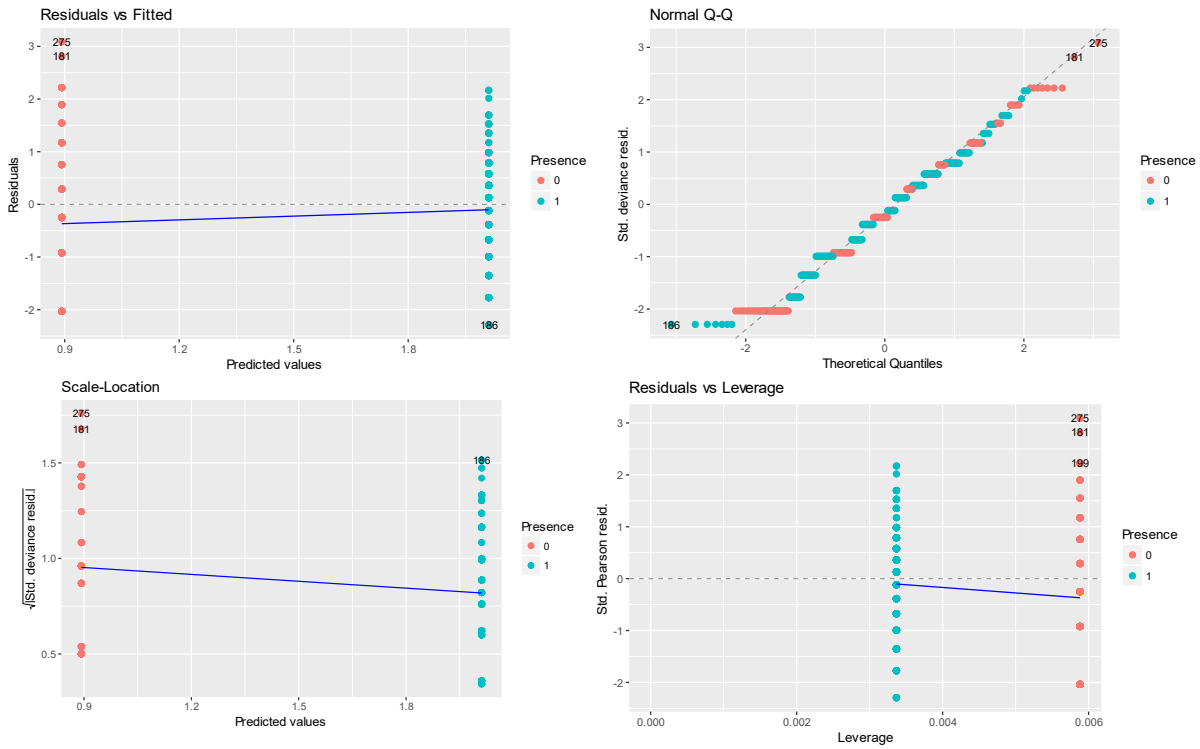

Fig. E6. Diagnostics of the GLM (species richness ~ presence).

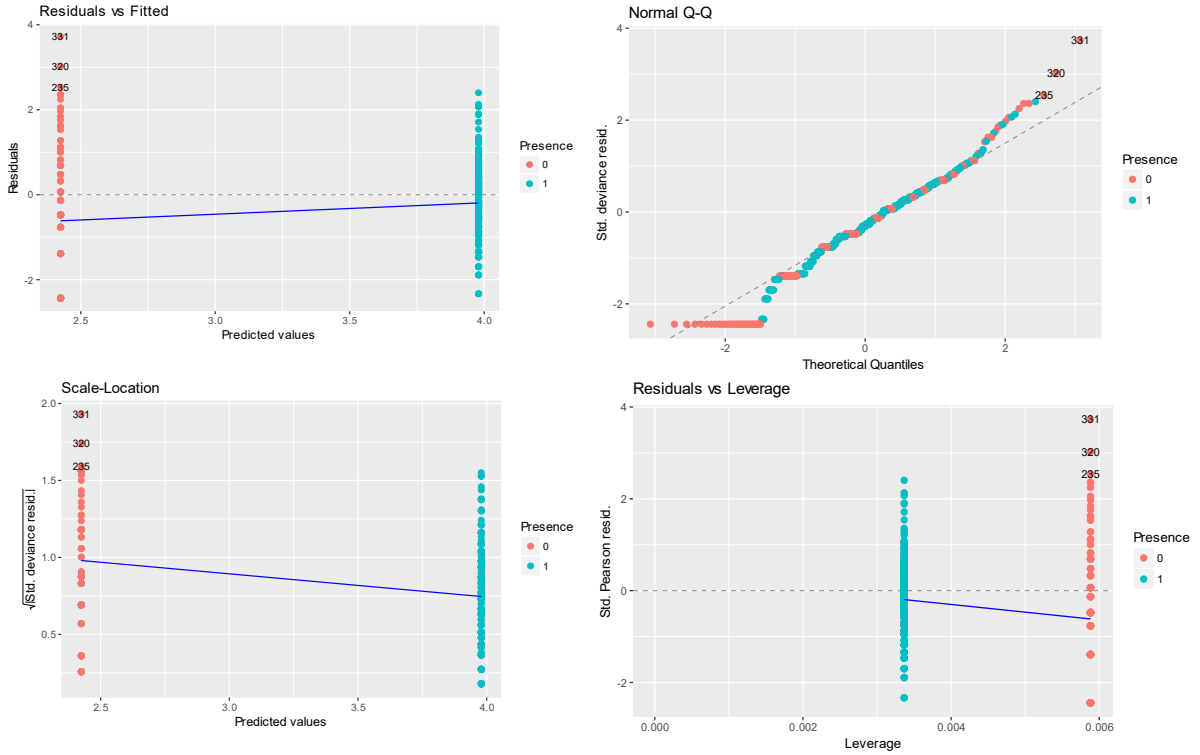

Fig. E7. Diagnostics of the GLM (abundance ~ presence).

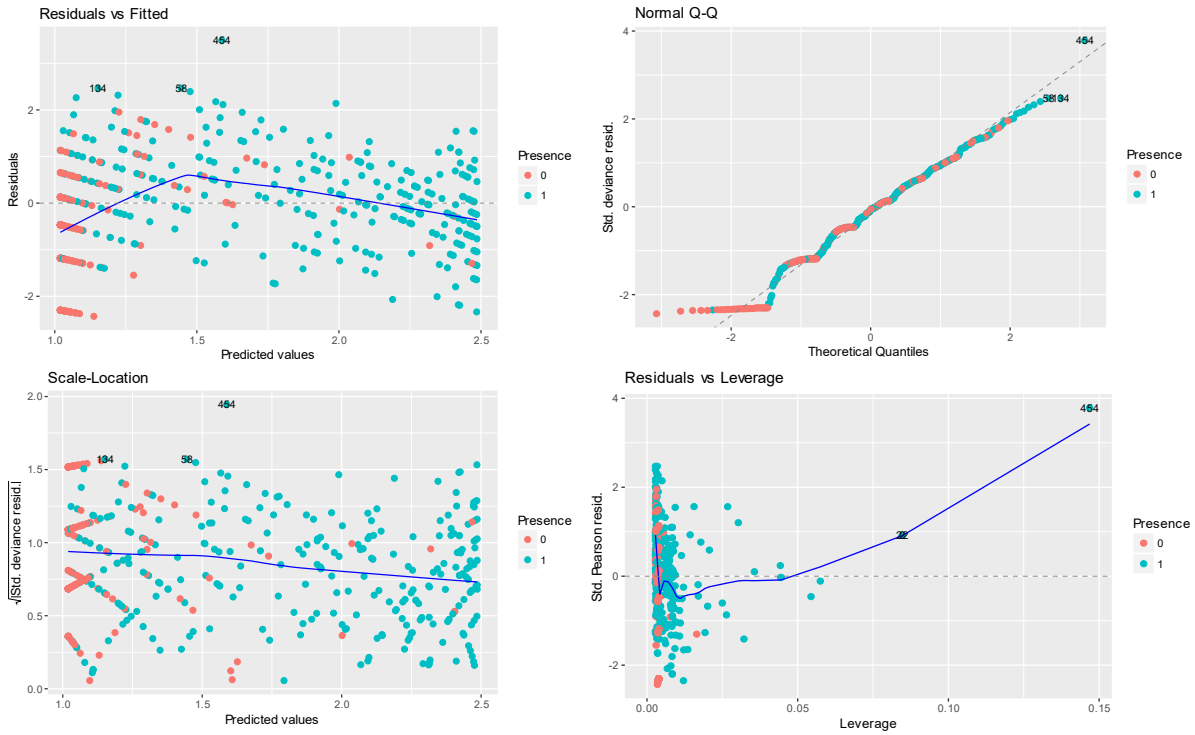

Fig. E8. Diagnostics of the GLM (species richness~poly(Cov,2).

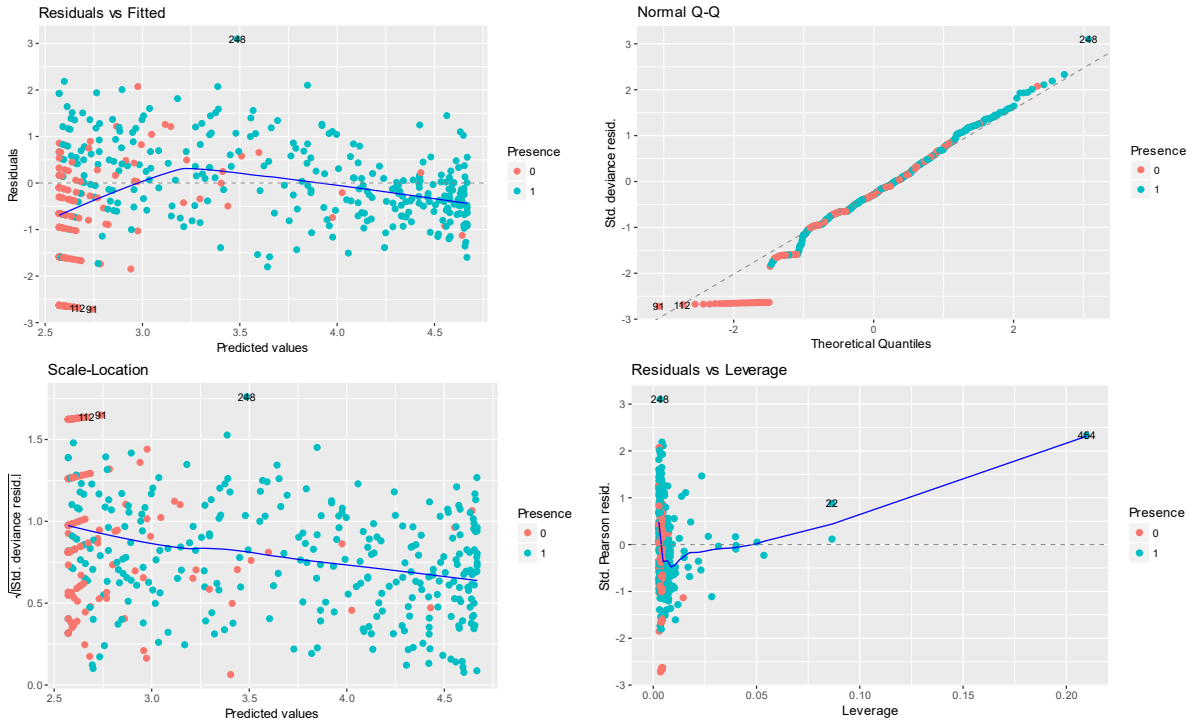

Fig. E9. Diagnostics of the GLM (Abundance ~poly(Cov,2).

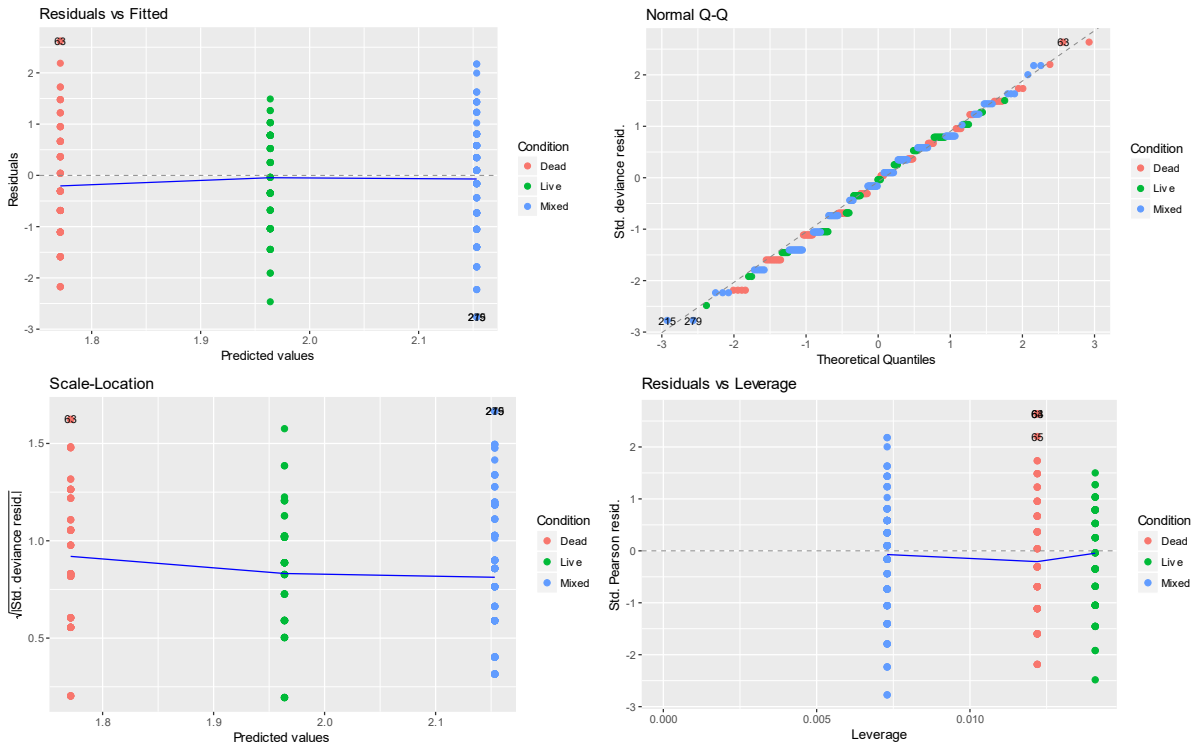

Fig. E10. Diagnostics of the GLM (species richness ~ condition).

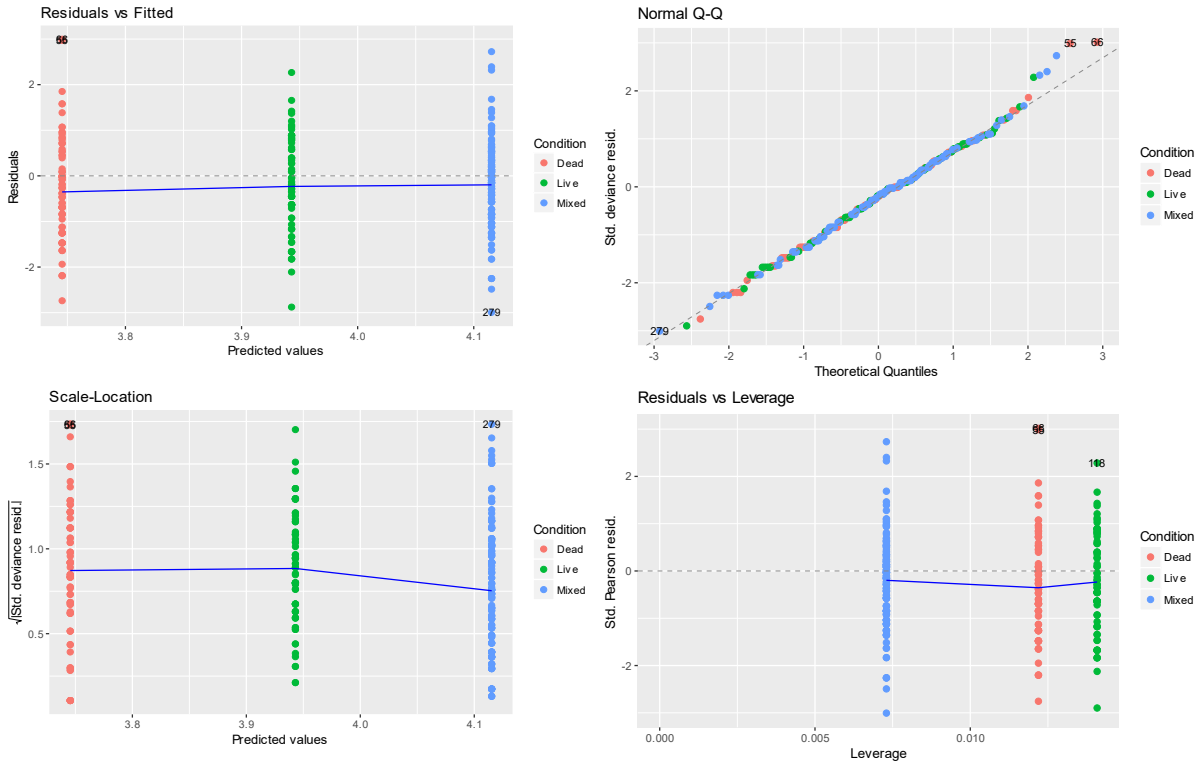

Fig. E11. Diagnostics of the GLM (abundance ~ condition).

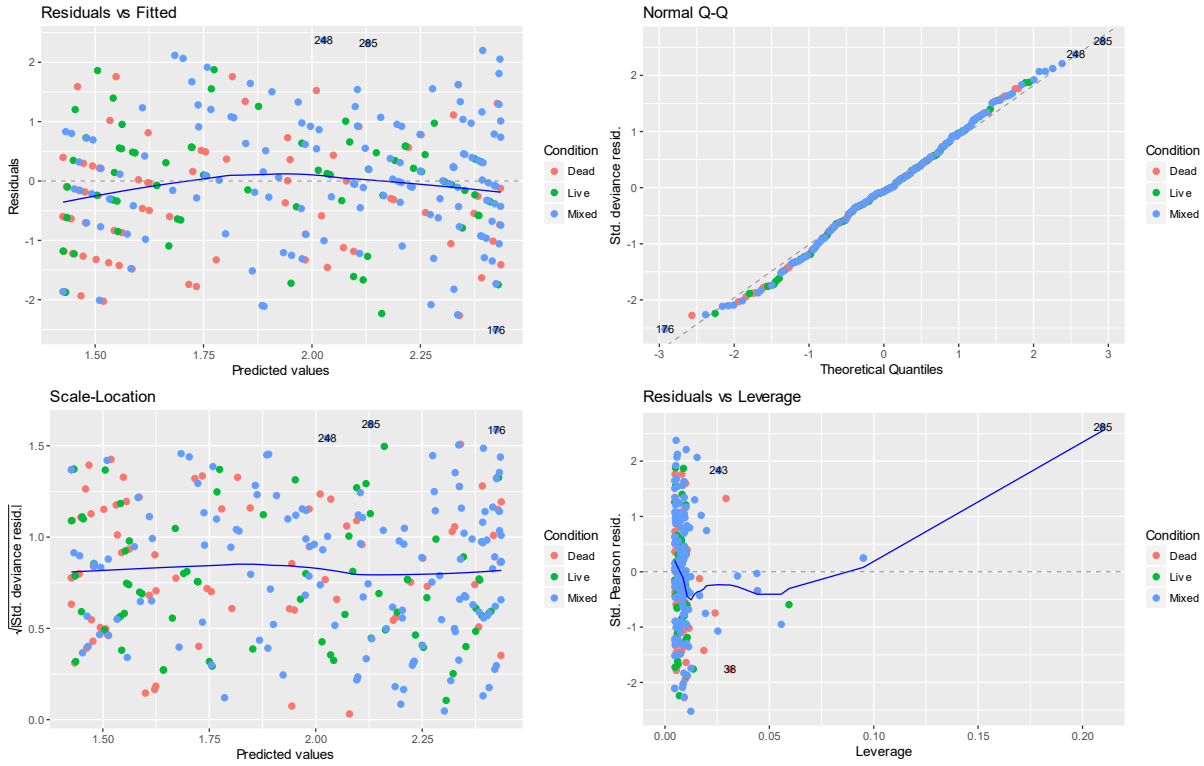

Fig. E12. Diagnostics of GLM (species richness ~poly(Cov,2)

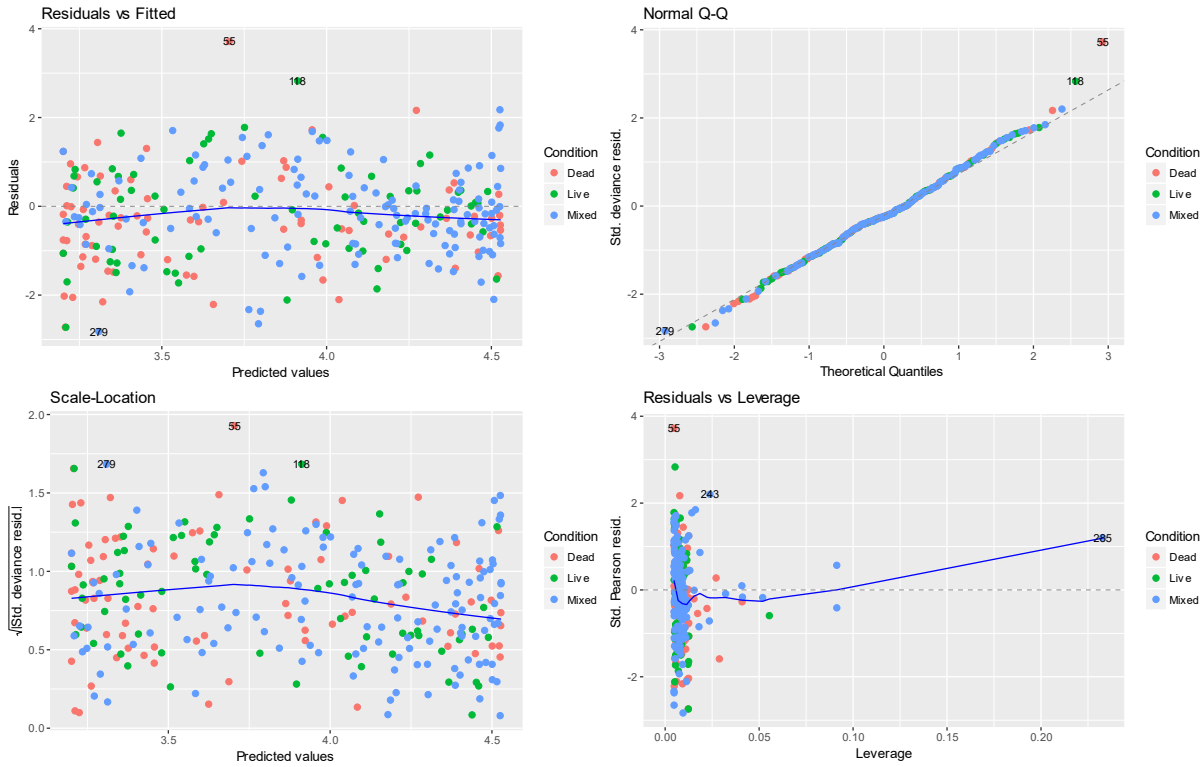

Fig. E13. Diagnostics of GLM (abundance ~ poly(Cov,2).